

**From standing posture to vertical
jump**
-
**Experimental and model analysis
of human movement**



Alice Palazzo

DIME-Department of Mechanical, Energy, Management and
Transportation Engineering

University of Genova

Dissertation submitted for the degree of

Doctor of Philosophy

27 March 2019

Acknowledgements

Se Willie Coyote ci ha insegnato qualcosa è che la determinazione, l'impegno, la pazienza e la preparazione non servono a nulla.

'Il coyote vive in un ambiente caratterizzato da una Natura malevola, un protagonista che senza fine, senza stancarsi, disastrosamente persegue uno scopo(...) molto molto meno di valore dello sforzo e delle risorse che il protagonista mette nel perseguirlo. L'oggetto perseguito - uno scheletrico e spolpato uccello - è meno di valore dell' energia, della concentrazione e delle risorse economiche spese dal coyote sul processo del perseguimento.

Perchè il coyote non prende i soldi che spende in travestimenti da uccello, catapulte, mangime radioattivo per Beep Beep e missili esplosivi e semplicemente non va a mangiare cinese?'

-D.F.Wallace-

I tre anni di dottorato sono stati una grande occasione di scoperta, impegno e dedizione per uno scopo incerto. Le sorprese e le conferme più importanti di questo periodo sono state le persone che mi hanno accompagnato, sostenuto ed aiutato durante il mio percorso. In primo luogo i miei **genitori**, che mi hanno insegnato la curiosità e la determinazione nel portare avanti i miei interessi senza pormi limiti. Le mie sorelle **Irene** e **Beatrice** che vicine o lontane sono sempre state compagne e amiche nelle mie scelte, sebbene sostengano che io abbia una "twisted mind".

Mattia che mi ha supportato nei lunghi anni di studio, con cui parallelamente allo studio abbiamo cresciuto i nostri bambini **Francesca** e **Michele**, mi ha concesso il tempo per portare avanti le mie passioni e si è preso il tempo per coltivare le sue in modo da rimanere persone attive e appassionate nonostante gli impegni di tutti i giorni.

Valentino, Benedetta, Francesca, Erika, Martina, Alice e tutti gli amici del liceo che mi hanno insegnato cosa sono delle vere amicizie, l'importanza di coltivarle e la felicità di ritrovarle anche dopo lunghi periodi.

I miei supervisori prof. **Francesco Crenna** e prof. **Giovanni Rossi** che mi hanno guidata nell'organizzazione del lavoro e sono stati esempio di dedizione per la conoscenza e la condivisione di quel poco che riusciamo a conoscere nelle nostre vite, la didattica. Un esempio di curiosità, precisione e perseveranza che non si smorzano nel tempo.

Giovanna, Barbara e Aiko che sono state di enorme aiuto come amiche e come ricercatrici, per tirarmi su il morale nei momenti difficili che attraversano tutti i dottorandi, per discutere di ricerca sociale e progetti di ricerca di grande interesse, ma soprattutto dagli acronimi significativi, non ultimo il fallimentare Horizon 2020. Avere delle amiche colte, divertenti e intelligenti è un grande privilegio e conforto.

Vorrei ringraziare i ragazzi dell'Emaro-Lab, Emaro-Club, Emaro-Bar che hanno condiviso i pranzi, i progetti, i dubbi, le frustrazioni, le distopie, i mondi dalla fisica distorta. Aspetto con trepidazione la creazione de "La StartUp" dove ci ritroveremo a lavorare tutti insieme, in una sede futuristica con progetti rivoluzionari. Grazie **Andrea, Alessio, Roberto, Alessandro, Kourosch, Luca e Mattia** che oltre ad essere colleghi sono amici, perchè come ho riso con voi non ho mai riso.

Grazie **Alvise** per l'ultima rilettura, per il tempo e per tutti i consigli.

Fletto i muscoli e sono nel vuoto

Contents

1	Introduction	1
1.1	Thesis structure	2
1.2	Personal contribution	2
2	Problem statement: Balance for human movement	4
2.1	Balance	4
2.2	Ankle and hip strategy	5
2.3	Measuring techniques	6
2.4	Modeling in biomechanics	11
2.5	Protocols	14
3	Proposed human model	18
3.1	The model	18
3.2	Reference system	19
3.3	Marker set	20
3.4	Inverse and Forward Dynamics	24
3.5	From markers to the model: approximations and problems	25
3.6	Instantaneous center of rotation	26
3.7	Solution of kinetics equations	34
3.8	Single degree of freedom analytical solution	36
4	Experimental set up: Measurement system and processing	38
4.1	Force plates and vision system	38
4.2	Laboratory calibration	40
4.3	Trigger	40
4.4	Acquisition and Elaboration Software	41
4.5	Experimental Protocol	43
5	Model validation: Identification methods and simulation	44
5.1	Identification	44
5.2	ARMA model	46

5.3	Identification algorithm	46
5.4	Simulation	50
5.5	Results	51
6	Model development: Dynamic balance	53
6.1	Ankle rotation	53
6.2	Weight Lifting	61
6.3	Squat jump	67
7	Conclusions	74
A	Simulators	78
A.1	OpenSim	78
A.2	Simulink	80
B	Software	84
B.1	Smart Capture	84
B.2	Sapera CamExpert	84
B.3	Acquisition software	87
B.4	Elaboration software	89
	References	99

List of Figures

2.1	Unperturbed standing (a), ankle strategy (b), hip strategy (c) combined strategy (d)	6
2.2	Load Cell	8
2.3	Force Plate	9
2.4	Wireless IMU	11
2.5	Models in biomechanics	16
2.6	Muscle model	17
2.7	Muscle curves	17
3.1	Model	19
3.2	Reference System	20
3.3	Angles conventions	21
3.4	Marker set	22
3.5	Experimental data	28
3.6	Synthetic data	29
3.7	ICR methods results	30
3.8	Result of ICR calculation body 1	31
3.9	Result of ICR calculation body 2	31
3.10	Reuleaux method	32
3.11	Velocity method	33
3.12	First body	34
3.13	Second body	35
3.14	Model	36
4.1	Gaitlab at 'La Colletta' Hospital	40
4.2	Signal flow	41
4.3	Trigger circuit	42
5.1	Reconstruction of auto-oscillating signal	51
5.2	Simulation of auto-oscillating signal	52
6.1	Foot model	54

LIST OF FIGURES

6.2	Forces acting on foot	55
6.3	GRF components in vertical (Y) and anterior-posterior (X) direction	57
6.4	Metatarsum, COP and ICR	58
6.5	Ankle moments measured according to different approaches	59
6.6	Ankle moments measured according to different approaches	60
6.7	Angular kinematics	62
6.8	Ankle angle comparison with or without shoes	64
6.9	Total COP comparison with or without shoes	65
6.10	Forces comparison with or without shoes	66
6.11	Subject during test	69
6.12	Vertical forces in jump	71
6.13	Mechanical Power measurement	72
6.14	Mechanical Power Peak	72
6.15	Mechanical Energy measurement	73
6.16	Potential Energy measurement	73
A.1	OpenSim front panel	81
A.2	Simulink Block Diagram	82
A.3	Simulink Simulation front panel	83
B.1	Smart Capture - Reference camera recording	85
B.2	Smart Capture - Force Platform	85
B.3	Sapera Cam expert software.	86
B.4	Front panel of the acquisition software	87
B.5	Flow diagram of elaboration software	89
B.6	Marker tracking flow diagram	91
B.7	Marker routine flow diagram	92

Chapter 1

Introduction

Biomechanics is the science that examines forces acting upon and within a biological structure and effects produced by such forces.

The field of "analysis of movement" describes one of the main human activities, in its variety from walking to weight lifting or athletes' performances.

The level of detail and complexity of the description is dependent on the goal of the study.

The study of mechanical characteristics of the human system is a widely explored field, because of the large amount of information that the study of simple and common gestures, like standing or walking, provides about the behaviour and the health both of the musculoskeletal and neurologic systems (13).

For clinical applications biomechanics lets the operator to analyze the system and synthesize the functions for rehabilitation and prosthetics. For sport application it permits the improvement of athletic performances through the optimization of training and specific equipment (27).

In engineering the study of movement and of the behaviour of human body is also related to anthropomorphic robotics, for example to mime the limbs. Biomechanics studies the mechanical characteristics of tissues to create prosthetics and to replace damaged body components too (50).

In the balance field many approaches have been used: considering biomechanical aspects, sensory and neural control aspects and the combination of both of them, but a lot of work has still to be done to understand the mechanisms that allow human bodies to maintain bipedal posture in everyday activities.

Biomechanical studies are often based on models, in fact a large set of quantities are not directly measurable and a model is required to estimate their values. The models accuracy has to be evaluated and the models have to be validated before using them.

The present work aims to study the insights of dynamic behaviour of human systems to maintain dynamic balancing, during the execution of gestures like,

for example, hopping, walking and jumping. The models developed have been studied to verify their boundaries of application and their reliability for different applications.

This thesis presents the study of static and dynamic aspects of human movement under a pure mechanical aspect and the evolution of the model used, due to the increasing complexity of the gesture analyzed. A particular attention is given to the measurement systems and the analysis of the variables and parameters involved in the modeling procedure.

1.1 Thesis structure

The thesis is organized as follows.

Chapter 2 Presents the problem of human stability, the studies already made in this field, the most used measuring techniques in biomechanics, the protocols and the models they are related to.

In Chapter 3 is depicted the model developed for the study of human stability, the protocol used and the marker set.

Chapter 4 deals about the measurement system designed and developed.

In Chapter 5 the algorithm of identification of mechanical parameters are described and results of the elaborations of trials are shown. In the same chapter the results of the simulation of a biomechanical system based on the model and the characteristics obtained from identification are presented.

In Chapter 6 other gestures are studied and models are modified respect to the characteristics of the gestures.

Chapter 7 contains concluding remarks and discussion for future work.

1.2 Personal contribution

My work has been mainly focused on the development of the measurement system, the analysis and the design of the models. Furthermore I did the trials on subjects for the different gestures, improving protocols prescriptions while I

1.2 Personal contribution

encountered criticalities in developing the elaboration data software. Then I developed the software to calculate the parameters we were interested with different identification methods of the parameters of the system. I used an Identification algorithm to obtain the values of these variables and then I fed the model to validate the results with a simulation.

In addition, I actively contributed to the software design and development. In particular, I worked on the simulators (**Appendix A**) and on Data management softwares (**Appendix B**).

Chapter 2

Problem statement: Balance for human movement

2.1 Balance

Humans are bipeds and two thirds of their body mass is located around two thirds of their body height. As a consequence the system is unstable unless a control system continuously acts: the balance control. In fact the center of mass is not perfectly aligned with the underlying articulations. The balance control is a complex system that involves different subsystems, like neurologic, somatosensorial and musculo-skeletal systems.

Different kind of locomotion drove the researchers to separate different field of study; standing on both feet is called sway, the study of balance during different movement is called dynamic balance.

The study of sway is a widely explored topic, both to understand the insight of human balance and to relate deviations from statistically normal indexes, to neurologic or physiologic diseases (51).

Maintaining balance in humans involve mainly four subsystems, controlled by the central nervous system: musculoskeletal system, vision system, vestibular system and somatosensory system(13).

The human vision system collects informations about changes in the environment, and the position of the body respect to them. The motor reactions to the stimulus sensed from the eyes are not fast enough to react to little, fast postural changes, so the main task of this system is to avoid obstacles and detect the best support for steps.

The vestibular apparatus is situated in the inner ear, it has the task to detect the movement of the head, acceleration and angular displacement. This apparatus lets us to sense the orientation of gravity. The dysfunction of the vestibular

system cause alteration of equilibrium, of ocular motility and has effects on the sense of orientation and on consequent dizziness and nausea.

The somatosensory system is composed of receptors distributed on skin, muscles, joint and inner organs; it is able to sense contraction and pressure and consequently the mutual displacement of body segment and the support surface.

The Central Nervous System (CNS) elaborates all the information collected by the three systems and the reaction is sent to the musculo-skeletal system to maintain the projection of the center of mass inside the base of support.

Control in balance can be proactive, like raise an arm or stepping laterally, or anticipatory in the case of well-learned perturbations like in gait or running. It can also be reactive, when perturbations are unexpected for the subject tested (39).

2.2 Ankle and hip strategy

The posture is the position of the body in the space. The principle which drives the assumption of a posture is to counterbalance the effects of external perturbations or gravity, with the minimum energetic cost. The reaction to a dynamic perturbation is called 'strategy' (16).

There are two main balance strategies, the first one doesn't involve the rotation of the hip joint and it is called 'ankle strategy', the second one instead comprehend the rotation of the torso around the hip and it is called 'hip strategy'.

The ankle strategy applies in quiet stance and during small perturbations, only the muscles of the ankle, plantar flexors and dorsi flexors act to control the posture (1). In more perturbed situations with higher velocities the hip muscles are activated to maintain the balance, flexing or extending hips and moving the Center of Mass (COM) anteriorly or posteriorly. There is usually a contemporary little activation of the muscles of every joint, but in great perturbations the effect on hip angle is considerably higher than in ankle strategy (21). Figure 2.1 illustrates the differences between the two strategies.

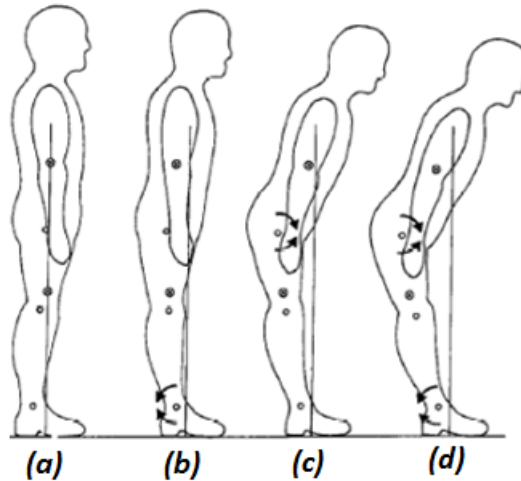


Figure 2.1: Unperturbed standing (a), ankle strategy (b), hip strategy (c) combined strategy (d)

2.3 Measuring techniques

In biomechanical studies, quantities under measurement can be divided in two classes: quantities related to motion characteristics, kinematic quantities, and quantities related to the forces who causes the movement, kinetic quantities. The forces cannot be directly measured so the only ones available are external forces. The quantities of interest in movement analysis are forces, footsole pressure distributions, accelerations, kinematics and muscle activity.

Forces

Human body is subjected to three forces: gravitational forces that act downward and are related to the mass; ground reaction or external forces that are distributed over an area of the body but they are supposed to act over a point called center of pressure and muscle and ligament forces that are the net effect of muscle activity.

The Center Of Pressure (COP) is the point location of the vertical reaction force vector. It represents a weighted average of all the pressures over the surface of the area in contact with the ground. When standing on two feet the COP lies somewhere between the two feet.

The forces that can be measured during human movement are external forces acting on the body or active forces and they can be directly measured in different ways: with strain gauges sensors and piezoelectric sensors.

Usually these sensors are mounted in multiaxial load cells. The preferred instru-

mentation to measure forces during human movement are force plates. There are also pressure forces, for example under the foot sole, but in this work the interest is focused on a overall force with an equivalent point of application.

Strain gauges sensors

Strain happens when a body deforms under the effect of some force, for linear elastic materials the relation between force and strain for a uniaxial loading condition is linear.

$$\sigma_a = E \cdot \varepsilon_a \quad (2.1)$$

where

σ_a is the stress

E is the Young's module

ε_a is the average deformation in direction of stress

The strain sensors exploit this property to transduce the deformation to a signal, the resistive transducers use the change in electrical properties of a wire stretched to measure the deformation of the wire integral with the structure.

Piezoelectric sensors

Piezoelectric transducers exploit the property of some materials, like quartz, to generate an electrical charge when subjected to mechanical strain.

Load cells

Load cells are transducers, which measure forces exploiting the knowledge of the geometrical and material properties of a deformable element. A load cell can be calibrated to determine the relation between the stress and the voltage output. Resistive transducers are mainly used for static force measurement, on the other hand piezoelectric ones are used for dynamic or quasi-static measurement.

Force plates

Force plates are rectangular plates supported at the four edges, in which there are vertical mono axial or tri-axial load cells to measure the modulus, the direction and the point of application of the force who acts on the plate. By using the

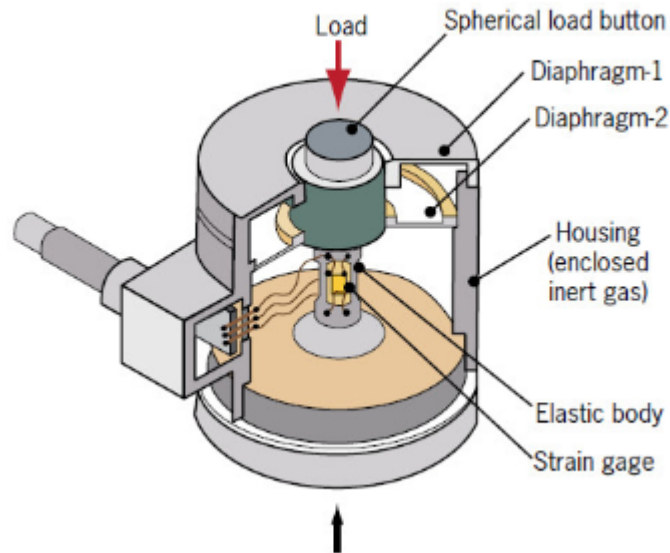


Figure 2.2: Load Cell

four vertical force components, that are usually the largest ones, considering the equilibrium of the plates for rotations it is possible to measure the equivalent point of application of the force on the force plate (COP).

Acceleration

Acceleration of a body can be measured by using sensors called accelerometers, often included in the wearable inertial sensors applied on a specific segment or by deriving two times the kinematic signal of a specific body point. This procedure, however, applied to the body could give a low quality measurement because of high pass effect of the derivation operation.

Kinematics

The study of kinematics of human movement requires the measurement of particular positions of the body in time. Usually each measurement is based on a predefined biomechanical model to identify the main degrees of freedom under study. According to the model, a set of anatomical landmarks are selected as the points of the body which movement has to be measured. They are mainly

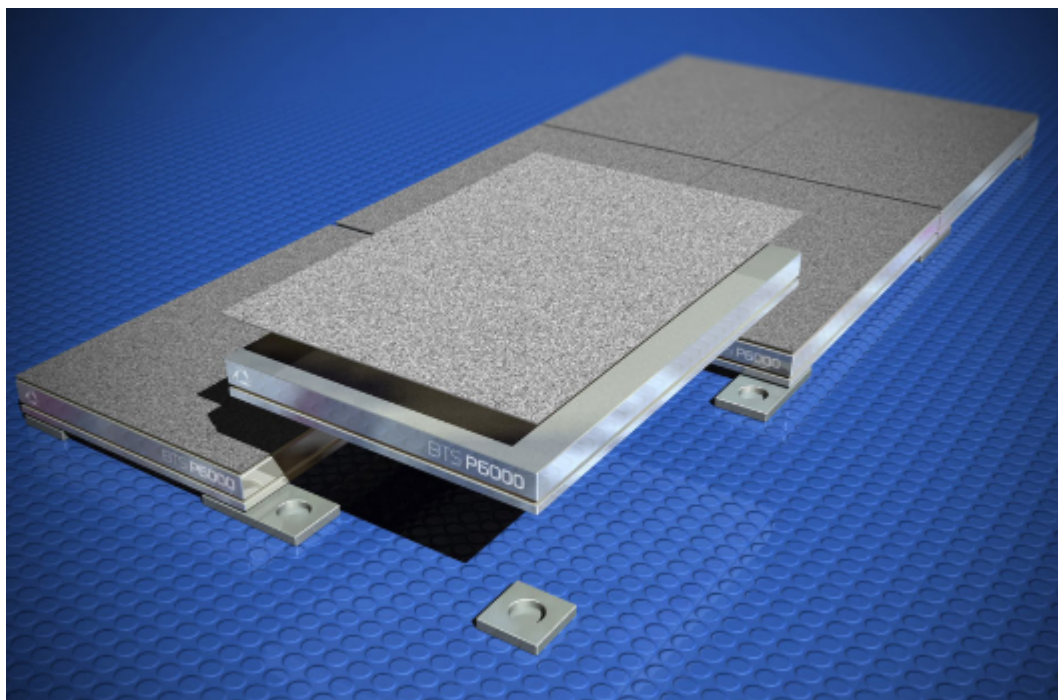


Figure 2.3: Force Plate

performed with optical methods or with inertial measurement unit (20).

Optical methods

Optical methods comprehend a markers-cameras system. Cameras are usually high-speed cameras, above 100 Hz frame rate, sensitive to a specific spectral region, like visible or infrared. Markers, which represent the points of interest of the recorded scene, can be active or passive, for example high intensity leds or reflective markers and printed figures. The main difference in these kind of markers occurs in software elaboration procedure, because of reflection or artifacts which occur in different situations.

Before the recording sessions, the system is calibrated to link the distance in pixels of cameras with the distance in millimeters. There are many characterisation with extrinsic and intrinsic parameters, and partial characterisations with just sensitivity parameters. For 3D set up the complete one is recommended because it is necessary to find the spatial relation between the cameras that constitute the points of view of the scene. For the 2D set up a partial calibration could be admitted if the alignment is accurated: a linear ruler, a chessboard or a stick with markers positioned at a determined distance, are sufficient only if the pixels

are squared, otherwise a cross ruler is needed (40).

The number of cameras depends on the nature of the gesture analyzed and on the used model, if the movement develops mainly in a direction, like walking (horizontally) and jumping (vertically), it is possible to use just a camera that project the scene on a single image plane. If the movement or the model used for its description is three dimensional, like throwing, it is necessary to have at least two cameras for multiple view processing of the scene. The commercial systems usually prefer to provide at least six cameras to be sure not to lose any markers due to occlusion from a body segment and to improve the accuracy of measurement, because the same marker is seen from differnt point of view and accuracy is better(Optitrack),(Vicon).

Inertial Measurement Systems

An inertial measurement unit (IMU) is a wearable electronic device that measure the orientation of the body to which is applied. It is composed of Micro Electro Mechanical Sensors (MEMS) that enable a significative dimensional and mass reduction as compared with traditional sensors. An IMU consists of: a gyroscope that measures angular velocity, a magnetometer that measures the magnetic field around the body, and an accelerometer. Each sensor is triaxial and gives informations referring to the same reference system. As a consequence to obtain the body position it is necessary to know the orientation between the sensor reference system and the segment reference system, where it is positioned.

This kind of sensors, in particular gyros, suffer for output offset drift which can cause an important error in measurement for long acquisitions (22).

Muscle Activity

Electromyography measures the muscular activity as the potential difference between two point of the same muscle. There are surface EMG and intramuscular EMG; surface EMG are restricted only to superficial muscles, and are influenced by the thickness of the tissue and cross talking between different muscles, but it is far less invasive than intramuscular EMG.

The signal obtained has to be elaborated, the information given from this kind of signal is better understood if the envelope of the signal is calculated (18),(19).



Figure 2.4: Wireless IMU

2.4 Modeling in biomechanics

Modeling is an attempt to represent a part of a phenomenon. The combination of modeling, experimental data and simulation is a powerful tool to describe in scientific terms the behavior of a specific property of a system. In biomechanics, modeling is a fundamental tool, in fact it is not possible to measure forces and torques at joint directly; to obtain these values it is necessary to perform an inverse dynamic procedure on the model.⁽³⁹⁾

Constructing a model needs the knowledge of the system or a set of experimental data. Using these data to arrive to a general model is an inductive and iterative process: a model needs to be validated and refined; the model resulting after this process is one of the possible models that can relate the inputs to the outputs.

The model is a simplification of the reality, in fact a wide part of the object modelled is neglected, if the results of simulations performed with the original model aren't consistent with the experimental data it is possible to change the assumptions made to describe it. The next step is to improve the model reanalyzing and considering some of the neglected aspect in the original model.

Each model must have parameters that can describe every meaningful change in the gesture.

First order models consider only bones and articulation, representing each body segment with a rigid body as first approximation, while the joints are modeled

as perfect mechanical joints. More complex models introduce the muscles in the behaviour of the biomechanical system, for example in OpenSim or Anybody, also for muscles a model is used to represent their mechanical effects.

Human body model for balance

In mechanics the human body is represented by segments linked by joints: the articulations. The segments are assumed to behave like rigid bodies. The most used model is composed by fourteen segments proposed by (13), in the case of quiet standing the models used are simpler, their peculiarities are described in the following.

The simplest one is a point model, that moves in the ground plane. The point is the COP and in this model, it is assumed that the COM correspond with the COP. Winter explained that the study of sway, indeed, refers to the relation between COM and COP.(30)

Norak and Nashner proposed two models able to catch the principal reactions of body to balance disturbance: the inverted pendulum, which is composed of a single segment linked to the ground, and the double inverted pendulum(49), which has two articulations at the ankle and at the hip to connect the two segments between them and to the ground. There are also more complex multi segmental models to describe specific gestures. See figure 2.5.

As in any model, the focus on a specific aspect depends on the application, clinical or biomechanical, and its goal: as an example in clinics the choice of a model depends mostly on the presence of a pathology in the study conducted, like for camptocormia in Parkinson's disease, hemiparesis, stroke, scoliosis and others. In research biomechanics the choice is driven by the application like prosthetics or exoskeletons.

The study of balance in quiet standing can be also modeled using the control theory, as a reaction of body control system to a perturbation (38),(17). In our study the neural control is blurred with the mechanical characteristics of the system.

In mechanics a rigid body is defined by three points not aligned, for this reason the data necessary to describe the body behaviour in space are the coordinates of these points. Data are collected with markers as described in section 2.3, the totality of these markers is called 'Markers set'.

It is important to underline that the model does not correspond with the markers set: it is possible to use different markers set for the same model, however there is a minimum number of markers in the set, defined by the model itself.

The main models used in balance studies are shown in figure 2.5, namely the

COP-COM model (points model), the simple pendulum model, the double pendulum model and the multi-segments model. A distinction method between models can be the plane in which the movement is studied, medio-lateral or anterior-posterior or both of them.

The human body can be modeled as a control system. The Central Nervous System (CNS), the controller, needs some knowledge about the system to be controlled. In the first years of growth of children the CNS learns to exploit the multiple degrees of freedom of joints, ligaments, muscles but also the kinematics and sensory redundancy to react to external stimulus with an appropriate adaptation of posture (41).

Mechanical properties

A mechanical model is constituted by a chain of rigid bodies, connected by joints, muscles and their effect drive the position and the mutual rotation between them.

Inertial properties of the human body

The inertial properties of human body mainly used for quantitative analysis in biomechanics are mass, the center of gravity and the mass moment of inertia.

To obtain these precise properties it is necessary to use instrumentation as computerized axial tomography or magnetic resonance imaging, but for general purposes they are too costly. In biomechanics the first experimental attempts to determine these values were made on cadavers, but also the definition of body segments didn't follow a common agreement, so the measure of these properties isn't standardized. In these studies about inertial properties of human parts, the assumption of homogenous distribution of densities is very rough, because the density of muscles, bones, fat and visceral organs are very different one to another.

The center of gravity had been measured with several methods, involving suspending or weighting body segments with 'ad hoc' instrumentations, which measure the moments at the stand points, knowing the mass of the part.

The moments of inertia are calculated with a pendulum or a torsional pendulum approach: after suspending the object in a fixed point, it is set in motion by few degrees and the time it takes for a period of oscillation is related to the moment of inertia.

All these studies have been reported to a statistic evaluation of these parameters, in fact some anthropometric tables have been produced to simplify this process of body characterisation.

Muscle model

The force-producing properties of muscles are nonlinear and complex, Ziac (1989) proposed a lumped-parameters dimensionless model. The entire complex of muscle and tendon can be modeled as a Hill type contractile element in series with a tendon.

The Thelen muscle model consists of a contractile element CE, an elastic parallel element PE and a series tendon element TE as shown in figure 2.6.

The force generated by a muscle respect to its length and to contraction velocity are shown in figure 2.7. The parameters to be known for each muscle are maximum isometric force, optimal muscle fiber length, tendon slack length, maximum contraction velocity and pennation angle (α).([OpeSimDocumentation](#))

Joint model

The articulations are represented, simplifying them, usually with planar or spherical joints. However, from an anatomical and geometrical point of view, real articulations aren't a perfect joint, they have some surfaces which slip one on another, this because these joints can't be naturally replaced, in this way the consumption of the biological tissue is distributed on the whole surface and not just in a single point, limiting the wear of cartilages.

As an example, the knee articulation, often modeled as a hinge joint, is a complex of roto-translational degrees of freedom.(27)

2.5 Protocols

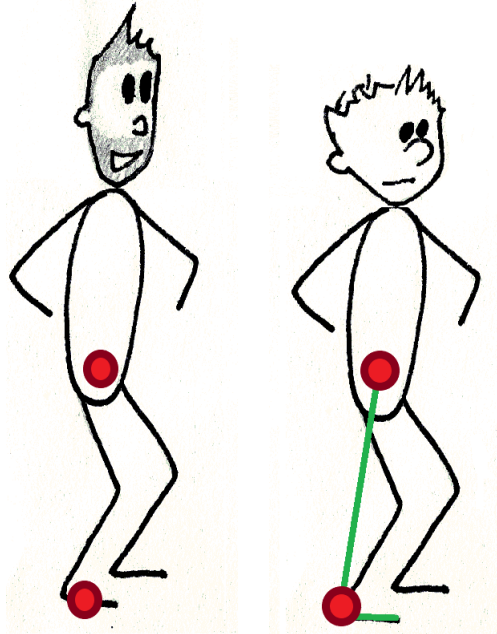
The study of balance needs a testing protocol to observe the phenomena. In literature there are studies which apply protocols devoted to observing natural sway and others about recovering balance after a perturbation.

Mechanism of quiet standing and perturbed standing are considerably different. To discover from a diagnostic point of view, a deficit of the systems, the response to a perturbation in standing is a more meaningful tool. It is also easier to separate the effects of the systems involved in balance control.

The perturbations could be internal, as the voluntary movement, or external, such as forces applied without the knowledge of the subject. In the first case there is a proactive response, so the CNS provides an anticipatory activation; in the other case, the movement of a platform, the pushes on arms, an inferior limb joint perturbation, or a perturbation on the trunk simulate an accidental perturbation of balance in which there is a higher latency of the motor control.

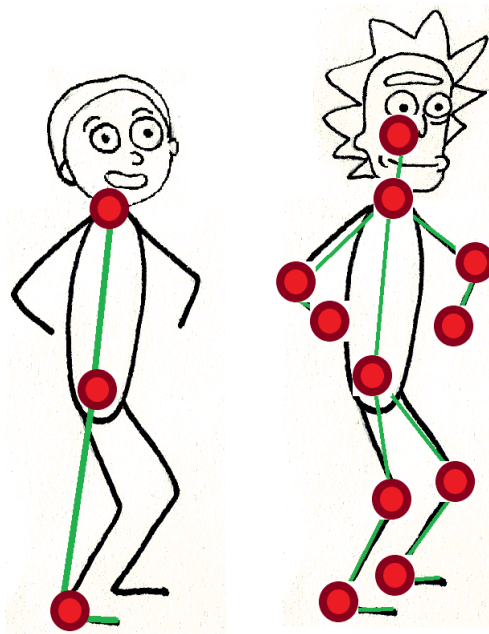
To ensure the repeatability and the reproducibility of measurements it is necessary to design a testing protocol: each subject has to be instructed about the assignments of the test, informed about the risks and the instrumentation used in the trial, the use and storage of data. The protocol must prescribe the instrumental set up, the calibration procedure and the elaboration procedure.

The design of a protocol permits to reproduce and verify the results of a study in other laboratories. In particular the behaviour of humans is variable and repeatable test condition influence the quality of measurements.



(a) *COP-COM.*

(b) *Single pendulum.*



(c) *Double pendulum.*

(d) *Multi segmental.*

Figure 2.5: Models in biomechanics

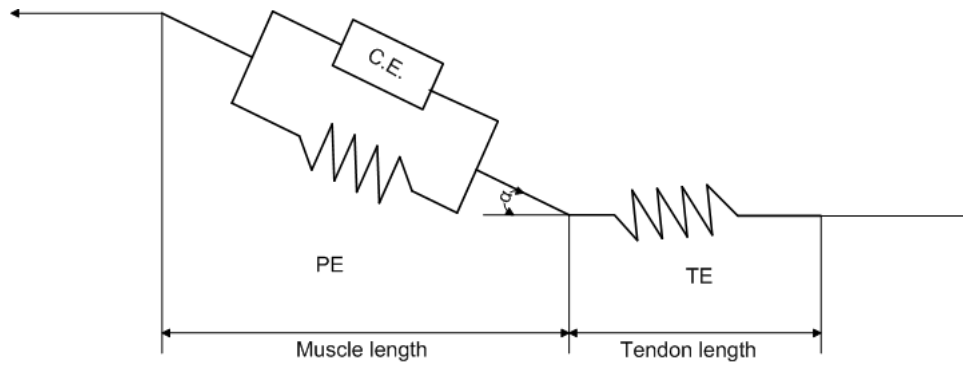


Figure 2.6: Muscle model

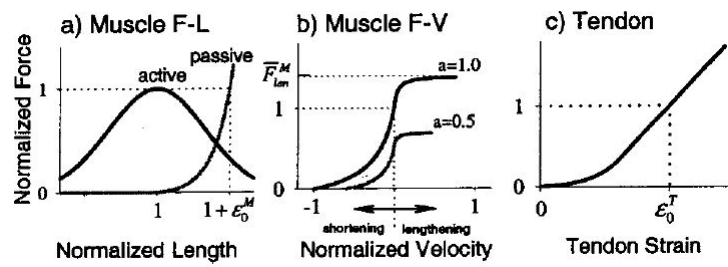


Figure 2.7: Muscle curves

Chapter 3

Proposed human model

3.1 The model

The model used in this first stage of development is a single degree of freedom inverted pendulum, used also in literature for example in (13) to study static standing.

Despite of that, during measurements we positioned more markers than the minimum required, so in the future the same data could be used to feed a multisegmental model as an evolution of the first approach.

The movements analyzed are mainly planar, as sway, walking, hopping and jumping at maximum height. They are also symmetrical on the mediolateral plane respect to the sagittal axis, so we assumed sufficient to monitor the movement of a single side.

We selected for simplicity of set up the instrumented leg to be the right one. As anticipated this model is very simple and its validity is debated in literature: main problems seem to be connected with the anatomical properties of the ankle and the inadequacy to describe the neuromotor control. Nevertheless this is a first order model and the information it provides, compared to its simplicity are really significative (37).

The model we are considering is a purely mechanical model in which also control characteristics are merged in the two dynamic parameters, stiffness and damping (34). We want to concentrate a mechanism in a position coincident with the ankle, which describe the control-biomechanics of the entire body-joint complex, regardless of the dynamic behavior of the whole body with the anatomy of the ankle (31).

In this multi-body model there are two segments, the foot and the body: the foot is linked to the ground assuming it never moves from it as depicted in 3.1. The body is connected to the feet with a hinge joint. The degree of freedom is just one, the ankle angle, given by the formula:

$$d.o.f = 3 * (n - 1) - 2 * c \quad (3.1)$$

Where

$d.o.f$ is the number of the degrees of freedom of the mechanism, in the plane
 n is the number of the bodies
 c is the number of hinge joints

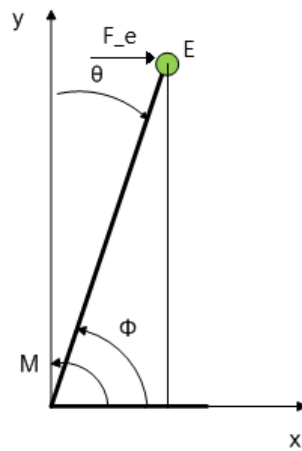


Figure 3.1: Model

3.2 Reference system

In biomechanics movement are studied referring to several reference systems. The Global reference system is fixed and defines the overall space where the movement takes place. The space in which the body moves has to be represented with a global reference system. Any local reference system or joint reference system has to refer to the global reference system.

The International Society of Biomechanics made standardization to make easier reading papers and the comparison between data sets(53). In this work ISB recommendations are followed.

There is a right handed orthonormal triad (X,Y,Z) with the origin in the ground, that in our case study corresponds with an edge of the force plates as shown in

figure 3.2.

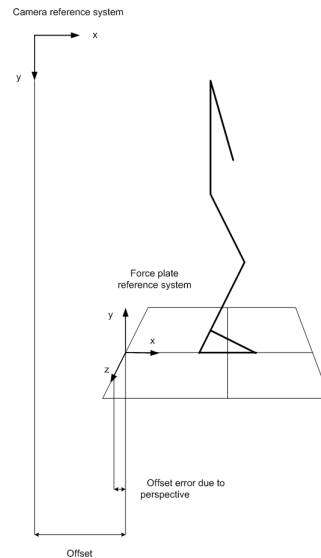


Figure 3.2: Reference System

The +Y axis is parallel to gravity and directed upward, X and Z axes lie in a plane perpendicular to it. If there is a clear direction in which movement develops, it is assigned the +X direction to it. In case of work on inclined planes, the reference system doesn't change definition and the X axis remains horizontal. Local reference systems can be associated with articulations or with segments or even with part of them. As an example for a segment of the leg, the local Y axis is positioned along the length of the segment, Z axis is on the mediolateral plane positive to right and the X axis is perpendicular, frontal and positive in the anterior direction. Definitions are referred to a segment of a body in standing posture.

Angles must also have a reference system and a positive direction. The null angle posture in the complete model is shown in figure 3.3, while the positive angle flexion is drawn in red in the same figure. We will call absolute segmental angles θ , angular velocities ω and angular accelerations α .

3.3 Marker set

Since we have positioned the markers on the articulation points, we can model the human body as a two segment planar structure. The first body, the feet, is

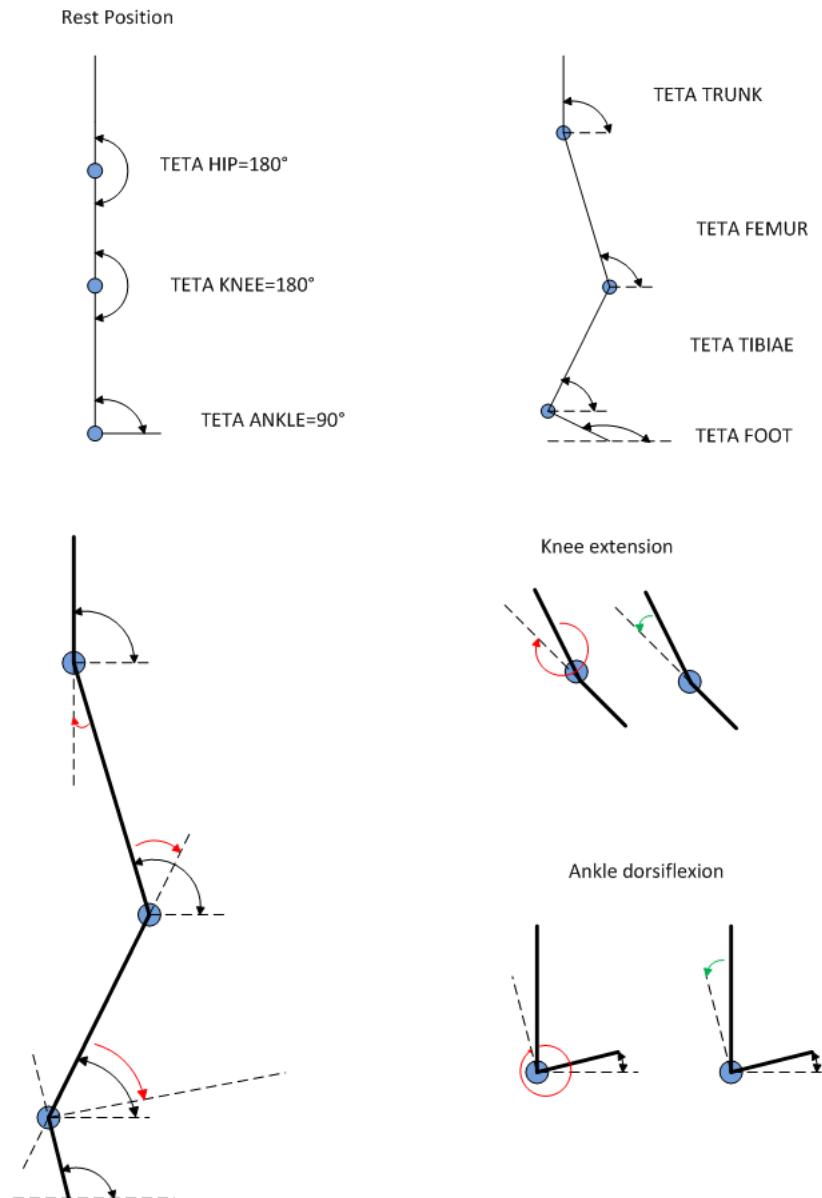


Figure 3.3: Angles conventions

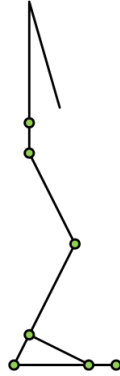


Figure 3.4: Marker set

bounded to the ground; the second one, the rest of the body, is linked to the first one with a hinge joint. The masses are obtained as a fraction of the total body mass, as tabled in anthropometric tables. CoM positions and moments of inertia are taken from the anthropometric tables, while the length of segments are instead measured directly on the subject.

In order to identify a segment, at least two markers are necessary. We decided to use four markers for the foot and two markers for each segment as shown in figure 3.4 and table 3.1.

We assumed to locate the Center of rotation of each joint at the anatomical landmark identified by the marker, because of the small amplitude of movement.

θ is the angle between the Y axis and the body, positive in clockwise direction. ϕ is the angle between the body and the foot, positive in counterclockwise direction.

x_f is the distance from the center of rotation of the ankle and the center of pressure of the foot.

x_c is the distance from the center of rotation of the ankle and the projection on the x axis of the center of mass.

Model parameters

Total body Center of mass

For a human standing upright, the center of mass could be placed ideally at the height of the iliac crest, or at the 53% of the total height of the subject, or it could be calculated as the weighted sum of the center of mass of each segment. (28)

Segment	Anatomical Landmark	Number
Foot	Malleolus	1
	Heel	2
	Metatarsum	3
	Foot tip	4
Distal leg	Ankle	5
	Tibiae epicondile	6
Proximal leg	Tibiae epicondile	7
	Femural great trochanter	8
Torso	Femural great trochanter	9
	Iliac crest/shoulder	10

Table 3.1: Anatomical landmarks for segments extremities

With each segment moving the whole body center of mass changes within time the position in the plane, its coordinates x_0, y_0 is calculated:

$$\begin{aligned} x_0 &= \frac{\sum x_n \cdot m_n}{M} \\ y_0 &= \frac{\sum y_n \cdot m_n}{M} \end{aligned} \quad (3.2)$$

Where

x_0 is the x component of the center of mass

y_0 is the y component of the center of mass

M is the total mass

x_n, y_n are the plane coordinate of each body's center of mass

m_n is the mass of each body

Moment of inertia

The value of the moment of inertia depends on the point around which the rotation takes place, and it is minimum when this point is the center of mass. Most body segments don't rotate around their centers of mass, but usually around an extremity. The relationship between this moment of inertia and that about the center of mass is given by the parallel-axis theorem(35).

$$I = I_0 + mx^2 \quad (3.3)$$

Where

I is the moment of inertia respect to the center of rotation

I_0 is the moment of inertia respect to the center of mass

m is the mass of the segment

x is the distance between the center of mass and the center of rotation

Often the values of inertia, gyration radius and the mass of each body part are available in the anthropometric table, as a percentage of total height or mass.

3.4 Inverse and Forward Dynamics

The model is the base for biomechanical investigation. The focus may be the description of kinematics or an investigation on the kinetic that generates movement. Regarding the forces the inverse kinetics has as inputs the movement and the external forces, and as outputs the internal forces and moments. Direct dynamics operates with the reverse logic. The validation of the performances of a model requires the use of both of them, generating at the end a simulated movement to be compared with the experimental one.

Inverse Dynamics

Inverse dynamics is a method to compute forces and moments of a kinematic chain, based on the motions of each segment composing the chain, the bodies' inertial properties and external forces. As the human body is modeled with rigid bodies, the external forces and the moments follow the rules of Newton-Euler equations. Main assumptions in inverse dynamics of human bodies is the stiffness of bones and the perfection of pivot joints, generating pure rotations around specific axes.

Forward Dynamics

Forward dynamics uses a mathematical model (mechanical equations associated with the model) to describe how the coordinates move due to the geometrical

3.5 From markers to the model: approximations and problems

properties, the constraints and the forces applied to the body.

From Newton's second law, we can describe the acceleration of coordinates as a relation to bodies' inertia and forces applied on it, as specified in 3.7.

Forces and moments in a biomechanical model are generated both from muscles and from external forces. The ones created by muscles act on kinematic joints as a torque, due to the point of insertion of the muscle on the articulation.

3.5 From markers to the model: approximations and problems

To pass from the real body to the model we have to make some assumptions that necessarily introduce an approximation error in the model. We said that we consider each segment as a rigid body. To identify a rigid body we need to measure three points not aligned and then create a reference system relative to the segment: the local reference system.

Anatomical landmarks

The local reference systems are defined by body surface markers, also called anatomical landmarks. An important issue in human movement analysis is the identification of these points and their reconstruction in the Global Reference System. Unfortunately anatomical landmarks are internal or under the skin and the determination of their location lacks of precision. This inaccuracy affects the estimation of joint kinematics and, consequently, kinetics.(11)

In this work we used the anatomical landmarks for planar movement that are most commonly found in literature.

One of the major source of error in finding the landmark position is the human error, that is the differences in the interpretation of the procedure of determination of anatomical landmarks. Other errors occur because the location is not a precise point, but often an irregular surface and there is a variable thickness soft tissue layer over it.

Soft tissue artifacts

Positioning of markers in optoelectronic stereophotogrammetry is not a errorless procedure because of the so called soft tissue artifacts (STA).

Inertial effects, skin deformation and displacement cause a marker movement

Joint	Anatomical Landmark
Ankle	Malleolus
Heel	Calcaneous
Metatarsum	Fifth metatarsal bone
Foot tip	Big toe
Knee	Tibiae epicondyle
Femur	Great trochanter
Hip	Femoral great trochanter
Shoulder	Acromion

Table 3.2: Anatomical landmark

respect to the relative bones. This artifact affects the estimation of skeletal kinematics and it is the most critical source of error in human movement analysis. This kind of skin movement is difficult to detect, even if it is greater than instrumental error: its frequency content is near to the frequency of the underlying bone, it depends on the movement taken into account and it varies between subjects. The frequency proximity of skin movement and bone movement doesn't allow to distinguish them through a filtering technique. A high number of studies reported the pattern and amplitude of soft tissue artifacts, the common conclusions are (26):

1. STA errors are usually larger than stereophotogrammetric errors;
2. STA pattern is task dependent;
3. STA is reproducible within, but not among subjects;
4. STA introduce both systematic and random errors;

3.6 Instantaneous center of rotation

Another approximation that introduces an error not negligible is the determination of the center of rotation of articulations. For a rigid body the instant center of rotation is the point around which the body rotates, usually its position changes during movement. If the body is constrained to rotate, the ICR coincide with the center of the constraint. The center of rotation is very important because we use it to define the rotation angles and we need the distance between

the insertion of the muscle and this point to obtain the force of muscles from the moment calculated with the inverse dynamic procedure.

Real articulations aren't a perfect hinge or spherical joints, they have some surfaces which slip one on another. The inaccuracies caused by the non-perfect rotation of the real joints are lower than the ones caused by the softness of body segments.

This implies that the center of rotation changes instant by instant and has to be determined. There are different methods to calculate approximatively the instant center of rotation, both in plane, ankle or elbow joint or in the three-dimensional space, hip joint.

ICR in human motion:

measurement and computational issues

Since the role of ICR in biomechanics is important we decided to investigate the measurement procedure to determine its positions, with a focus on metrological performances. Therefore, we consider its measurement, based on video image acquisition and processing of human motion records. Measurement and computational issues are discussed, including the evaluation of measurement uncertainty and the estimation of the effect of some influence quantities on the determination of the position of the instantaneous center of rotation.

A proper approach consists in a video based measurement system, including a set of markers placed in specific points along the body segments investigated.

Even if usually positions of a cluster of markers on each segment are measured, in this case we considered a minimum of two markers along each segment.

We confront the Reuleaux method previously described and the 'point velocity method', since at each time the point velocity can be evaluated with a Savitzky-Golay filtering. In this case ICR is located at the intersection of lines perpendicular to point velocities at each time.

Pure translation is an issue since it produces an ICR located at infinity. On the other hand a combination of linear translation and rotation will move the ICR. This is particularly interesting when translation is due to the joint under investigation, like, for example the knee.

We used synthetic and experimental data to evaluate measurement methods and the influence of measurement noise, chord length and pure translation. Synthetic data are useful to evaluate the processing techniques. It is possible to obtain synthetic kinematic data of a set of rigid bodies connected by pure revolute joints with the first ICR fixed or subject to a controllable linear translation. Beside that

3.6 Instantaneous center of rotation

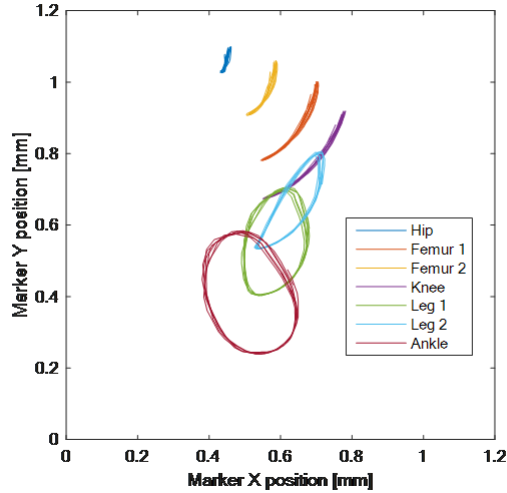


Figure 3.5: Experimental data

we can vary relative angular velocities and sampling frequencies and introduce some noise if required.

Figure 3.5 present markers trajectories for a pedalling leg while figure 3.6 present the trajectories of synthetic data of points of two rigid bodies. For synthetic data it is possible to vary linear translation, angular velocity and sampling frequencies. The two processing procedures have been validated with the synthetic data. The ICR variability is more evident in the second body computation, so we varied some computational parameters:

1. random Gaussian noise on position measurement;
2. length of chord;
3. number of point involved in calculation;

Concerning Gaussian Noise we have considered a std deviation of 0.5, 1.5 and 3 mm. These are representative of good, normal and difficult experimental set up and image processing. The length of chord is linear with rotational velocity and sampling frequency. A minimum of two points is required to calculate the ICR, but we used three points as often happens in biomechanical markers set up.

Figure 3.7 presents the standard deviation of ICR results as a function of the chord for three noise level, and three methods: the Reuleaux method, the velocity point with two or three points. It is possible to note that velocity methods are more stable when varying chord length.

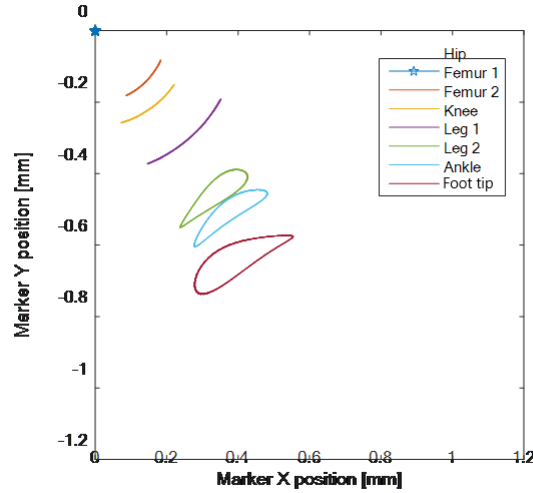


Figure 3.6: Synthetic data

The velocity method proved to be more reliable in presence of noise in particular when three markers are involved in the procedure. When a translation is added ICR measurement is very critical especially when dealing with the second segment in a two degrees of freedom system. We obtained some useful indications for the variability of the results and its dependence on noise and chord length or sampling rate. The velocity method has demonstrated a very good stability with both noise and chord length variations as compared with the original Reuleaux's method. Nevertheless, when dealing with the second body in a chain, uncertainties are very large and results become unreliable in the practical application considered.

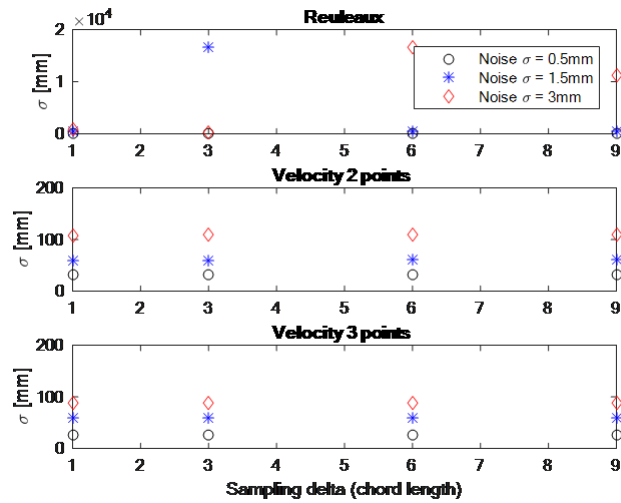
In this case some further investigation is required to confirm that a violation of the rigid body hypothesis causes unpredictable ICR position deviations and to determine if there are feasible countermeasures to limit such effects when processing the results.

The Reuleaux technique

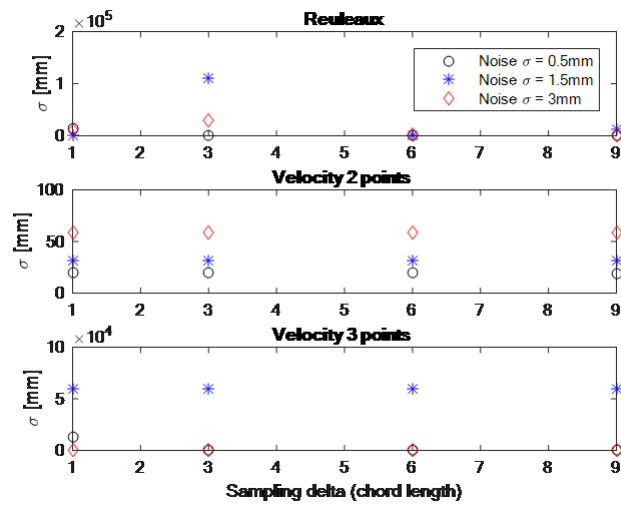
This ICR calculation technique is simple to use and very diffused for this reason. However it is susceptible to the magnification of errors for small angles of rotation and low angular velocities.

Consider a limb constituted by two rigid bodies connected by a hinge joint and the position of two points A and B at time t_i and t_{i-1} figure 3.10. The main hypothesis is that at each time the movement of a rigid body can be reconstructed

3.6 Instantaneous center of rotation



(a) Chord length 1.



(b) Chord length 2.

Figure 3.7: ICR methods results

3.6 Instantaneous center of rotation

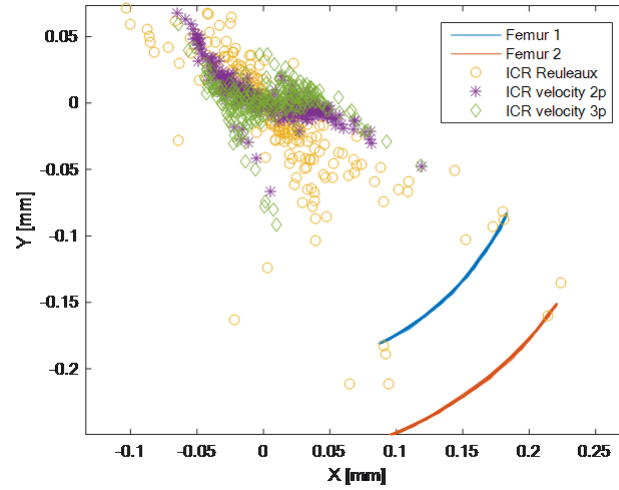


Figure 3.8: Result of ICR calculation body 1

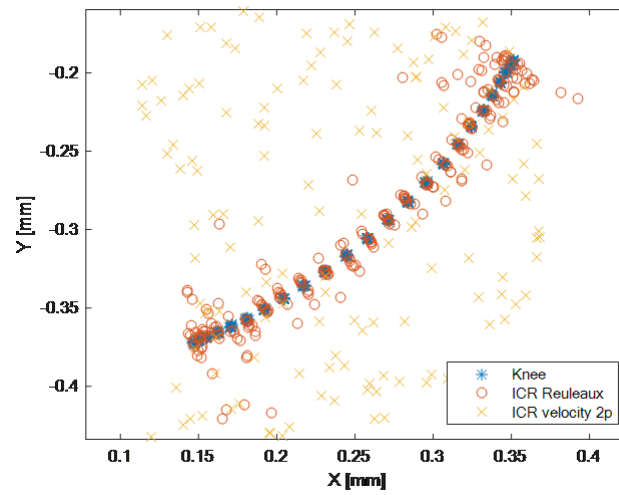


Figure 3.9: Result of ICR calculation body 2

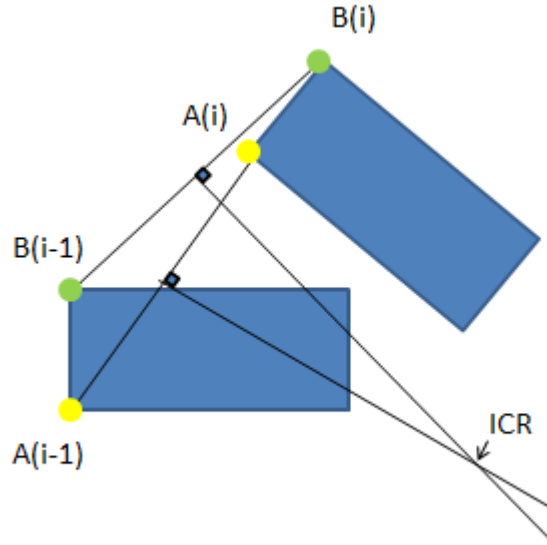


Figure 3.10: Reuleaux method

as a rotation around an ICR. So we can consider the segment connecting two subsequent positions of each point as the chord of a circumference arch actually connecting the same points. The ICR is located on the line perpendicular to the chord and passing to its middle point. If there are multiple points it is possible to obtain several perpendicular lines and their intersection is the Instantaneous Center of Rotation of the body.

Point velocity method

Considering a general plane motion of a body as in figure 3.11, at given instant, the velocities of various particles of the body could be expressed as the result of a rotation whose axis is perpendicular to the plane. This axis intersects the plane at a point called the ICR. If a line is drawn perpendicular to v_A , at A the body can be imagined to rotate about some point on the line. Similarly, center of rotation of the body also lies on a line perpendicular to the direction of v_B at B. If the intersection of the two lines is at I, the body will be rotating about I at that instant. The point I is known as the instantaneous centre of rotation for the body.

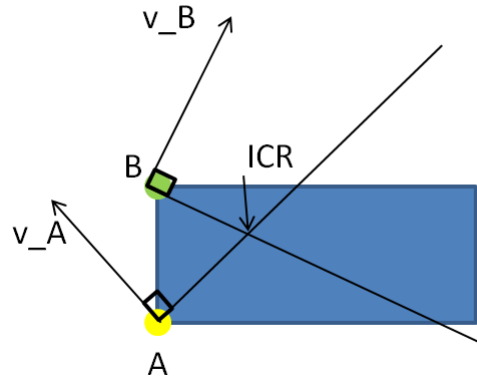


Figure 3.11: Velocity method

Functional method

Alternative approaches for CoR estimation have primarily been iterative. Other methods are functional methods, they use cost function minimization to fit marker trajectories to the joint model, Halvorsen et al. (1999), Gamage and Lasenby (2002), and Pratt (1987) use least-squares (LS) methods which give exact CoR estimation techniques. Halvorsen et al.(1999) adapts the Reuleaux construction for computing a single instantaneous CoR (Reuleaux, 1876; Panjabi,1979).

Iterative methods

The major disadvantage of these iterative approaches is the potential for different solutions depending on the existence of local minima in the cost function and values of optimization parameters such as convergence criterion, weights, and initialization.

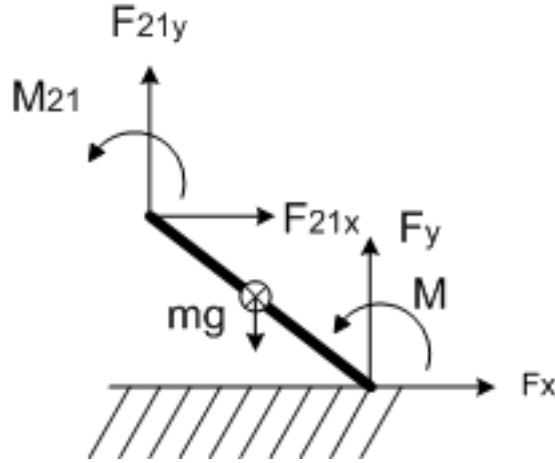


Figure 3.12: First body

3.7 Solution of kinetics equations

In this section the free bodies diagrams are solved and formulas of inverse dynamic are developed. The name of the forces specifies the direction of the force (x,y) , while the number (ij) means that the force acts from body i on the body j . l is the length of the segment. The quantities related to the body are indicated with j .

Forces and torques are calculated solving the equilibrium of the Newton-Euler equations:

$$\begin{cases} \sum F_x = m\ddot{x}_c \\ \sum F_y = m\ddot{y}_c \\ \sum M = J\ddot{\theta} \end{cases} \quad (3.4)$$

First body

For the first body, as shown in figure 3.12, forces are measured as ground reaction forces and they are F_x, F_y, M ; The moment exchanged with the ground, M , is null.

$$\begin{cases} F_{21x} + F_x = m_1\ddot{x}_1 \\ F_{21y} + F_y - m_1 \cdot g = m_1\ddot{y}_1 \\ M_{21} = J\ddot{\theta} + m_1 \cdot g \cdot x_1 \cos \theta_1 - [F_{21y}]l_1 \cdot \cos \theta_1 - [F_{21x}]l_1 \cdot \sin \theta_1 \end{cases} \quad (3.5)$$

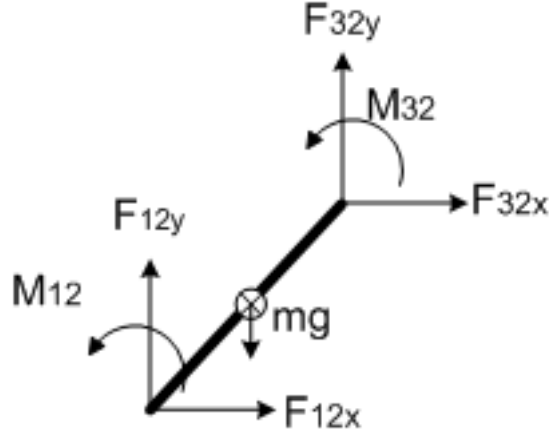


Figure 3.13: Second body

$$\begin{cases} F_{21x} = -F_x + m_1\ddot{x}_1 \\ F_{21y} = m_1\ddot{y}_1 - F_y + m_1 \cdot g \\ M_{21} = J_1\ddot{\theta}_1 + m_1 \cdot g \cdot x_1 \cos \theta_1 - [m_1(\ddot{y}_1 + g) - F_y]l_1 \cdot \cos \theta_1 + [F_x - m_1\ddot{x}_1]l_1 \cdot \sin \theta_1 \end{cases} \quad (3.6)$$

Second body and subsequent

To transfer the solutions of the first body to the second one, whose free body diagram is shown in figure 3.13, we have to introduce the interface equations:

$$\begin{cases} F_{12x} = -F_{21x} \\ F_{12y} = -F_{21y} \\ M_{12} = -M_{21} \end{cases} \quad (3.7)$$

And supposing there are no other forces applied we solve the equations:

$$\begin{cases} F_{32x} = F_{21x} + m_2\ddot{x}_2 \\ F_{32y} = F_{21y} + m_2(\ddot{y}_2 + g) \\ M_{32} = M_{21} + J_2\ddot{\theta}_2 + m_2 \cdot g \cdot x_2 \cos \theta_2 - [m_2(\ddot{y}_2 + g) - F_{12y}]l_2 \cdot \cos \theta_2 + \\ + [F_{12x} - m_2\ddot{x}_2]l_2 \cdot \sin \theta_2 \end{cases} \quad (3.8)$$

The process is iterative and allows to calculate moments and forces at every joint of the segmental structure.

3.8 Single degree of freedom analytical solution

As a reference, configuration of static equilibrium is shown in figure 3.14.

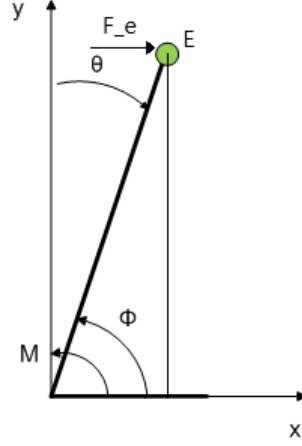


Figure 3.14: Model

The moment at the ankle is calculated as shown in previous section and the physical behaviour of the ankle complex is modeled as a rotational spring-damper system.

The moment created by the visco-elastic spring respect to the reference configuration is:

$$M = M_r - k_0(\theta - \theta_r) - c\dot{\theta} + M_d \quad (3.9)$$

Where

M_r, θ_r are the moment and the angle in rest position

While the equation of motion in this case is:

$$(J + md^2)\ddot{\phi} + mgd \cos(\phi) = M + M_e \quad (3.10)$$

Where

$$M = mgx_f$$

3.8 Single degree of freedom analytical solution

and

$$M_e = -F_e \cdot y_E$$

F_e is the external force applied to point E

and changing the free coordinate:

$$\phi = \frac{\pi}{2} + \theta \rightarrow \cos(\phi) = -\sin \theta \quad (3.11)$$

Equation 3.9 becomes:

$$(J + md^2)\ddot{\theta} - mgd \sin(\theta) = M + M_e \quad (3.12)$$

Then we introduce two approximations:

$$J \ll md^2; \sin \theta \simeq \theta \quad (3.13)$$

Equation 3.10 becomes:

$$md^2\ddot{\theta} - mgd\theta = M + M_e \quad (3.14)$$

In the reference configuration, supposed as a condition of static equilibrium we can describe the M_r , the moment at rest position, the position in which the projection of COM correspond to the mean value of sway oscillation, the term of equation 3.9, as:

$$M_r = mgd\theta_r \quad (3.15)$$

And substituting in 3.12

$$\begin{aligned} md^2\ddot{\theta} - mgd\theta &= M_r - k_0(\theta - \theta_r) - c\dot{\theta} + M_d + M_e \\ md^2\ddot{\theta} - mgd\theta &= mgd\theta_r - k_0(\theta - \theta_r) - c\dot{\theta} + M_d + M_e \\ md^2\ddot{\theta} + (K_0 - mgd)(\theta - \theta_r) + c\dot{\theta} &= M_e \end{aligned} \quad (3.16)$$

which becomes, with the definition of the parameters θ' and k :

$$\begin{aligned} \theta' &= \theta - \theta_r \\ k &= k_0 - mgd \end{aligned} \quad (3.17)$$

$$md^2\ddot{\theta} + k\theta' + c\dot{\theta}' = M_e \quad (3.18)$$

Chapter 4

Experimental set up: Measurement system and processing

In this chapter we consider the measurement systems used for experiments. They are related to Ground force, COP measurements and kinematic measurements.

4.1 Force plates and vision system

Measurement laboratory set up

The force plates used in the Measurement Laboratory of the University of Genoa are two BTS Bioengineering P 6000, mounted with a wooden walkpath to allow a dynamic gesture not to be influenced by the step between the ground and the surface of the force plate. The overall length of the walking path in the laboratory is about 4.5 m so it is long enough to enable walking analysis. Nevertheless, a longer distance could stabilize the gait cycle as it happens in 'La colletta Hospital'. The P6000 metrological characteristics are listed in the table [4.1](#)

The outputs of the force plate are tridimensional data of forces and COP position on the platform plane.

Acquisition from these sensors are made with a proprietary software: Smart Capture (description in appendix [A](#)).

Data can be exported to a text file, easily importable in Matlab.

The camera is a Falcon Dalsa 1.4M 100XDR series. It acquires images in grayscale, 16 bits at 100 Hz, and it is mounted on a fixed support to maintain the calibration.

4.1 Force plates and vision system

Dimensions	600 · 400 mm
Range	2000 N
COP spatial resolution	1 mm
Sampling Frequency	1 kHz
Resolution	16 bit
Deviation from sensitivity	< 1% range
Linearity	< 0.2% range
Hysteresis	< 0.2% range
Mass	28 kg

Table 4.1: BTS P6000 characteristics

The video acquisition board is the Xcelera X64-CL LX1 and it is managed by the Sopera Cam expert software (description in appendix A).

Sopera drivers give the camera access to Matlab, so I have developed a image acquisition and processing sw in Matlab environment to avoid a mixed approach between Sopera and Matlab. It is possible to create a configuration file, in which are specified the necessary settings to the camera for working properly. This configuration file is readable by the Matlab Imaq Tool and so it is possible to manage the camera from Matlab software.

In order to capture the points of interest of the subject, seven high intensity leds are fixed in histhe anatomical landmarks of the subject.

Measurements of COP are made with the force plates and COM ones are made with the camera-markers system. To confront the two measures it is necessary that they share the same reference system. In this case we have the force platform which provides tridimensional informations and the camera which provides a planar measure.

'La Colletta' Hospital set up

The hospital 'La Colletta' located in Arenzano, Genova has a "Gait Lab" facility: the BTS GAITLAB (BTS S.p.A., Milano, Italy). The laboratory in figure 4.1 is composed of two force plates surrounded by a wooden walkpath, whose overall length is about eight meters, six infrared camera and sixteen superficial electromyographic probes. Each measurement system is integrated and managed by the proprietary software (description in appendix A), Smart capture, Smart



Figure 4.1: Gaitlab at 'La Colletta' Hospital

tracking and Smart analyser software. Furthermore, for clinical use, a set of protocols are available and the user is guided in their use by the Smart clinic environment.

The outputs of the "Gait Lab" are tridimensional data of forces, the measurement of the COP, tridimensional position of each marker and the electromyographic signal of each probe. Signals are saved in a proprietary file format and can be exported for a further Matlab elaboration.

4.2 Laboratory calibration

To pass from the measure in pixels to the measure in millimeters, we created a calibration protocol. A beam, 1200 mm long, is marked at intervals of 100 mm. An image is taken and the sensitivity of the camera is obtained with a linear regression.

Measurement procedure do not permits to position the feet in a precise point of the platform and plane of the calibrated space nor to measure it before taking the sway measurement, because it is necessary to restart the force platform for each test. So we take the result of Winter as an assumption: even if there are differences in amplitude and phase in the signals of COP and COM, their mean value, for a few seconds long signal, is the same. For each trial, we measure the offset between the camera and the force plate as shown in figure 3.2.

4.3 Trigger

The two calibrated measurement systems have now to be coherent also from a timing point of view. For this reason the systems have to start in the same

4.4 Acquisition and Elaboration Software

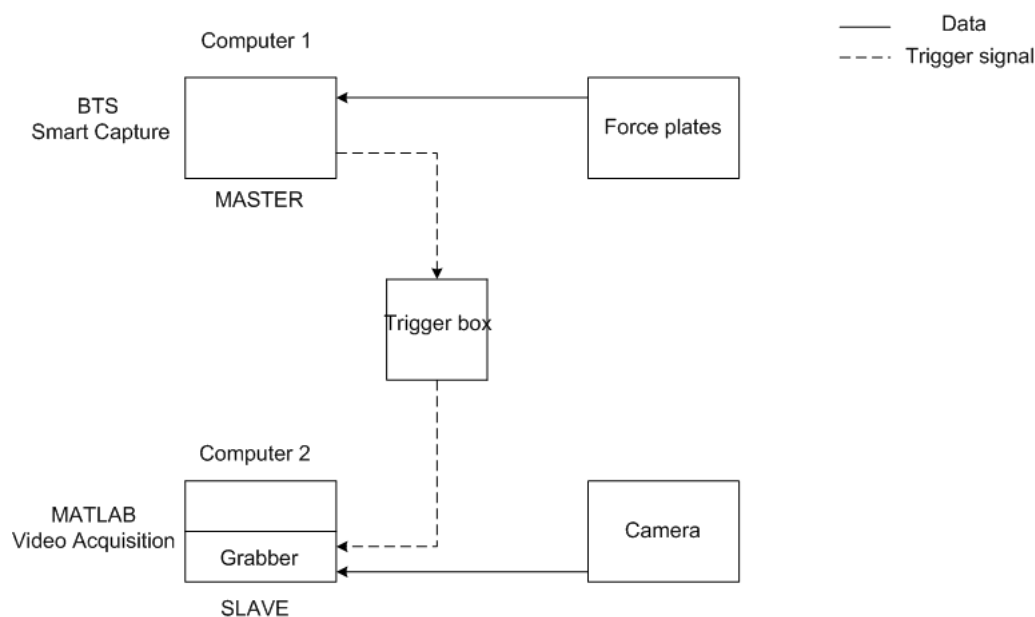


Figure 4.2: Signal flow

instant of time. The software that controls the acquisitions is able to produce a trigger signal, while an hardware, the camera grabber accepts a trigger input. The trigger signal to whom the grabber is sensitive it is a 10 V falling edge signal, while the signal generated by the trigger box is a 3 V signal. It has been necessary to create a level adapter circuit to provide the correct signal as shown in figure 4.2.

4.4 Acquisition and Elaboration Software

The software we use has been developed in our laboratory in the Matlab environment. The libraries belong to the Image Acquisition Toolbox. We did not use the embedded tool because we needed to set some features that weren't included in the guided image acquisition interface and we wanted a custom system with specific options and requirements. Elaboration software calculates markers' kinematics from the video of the trial recorded with the Acquisition software. They are further described in appendix B.

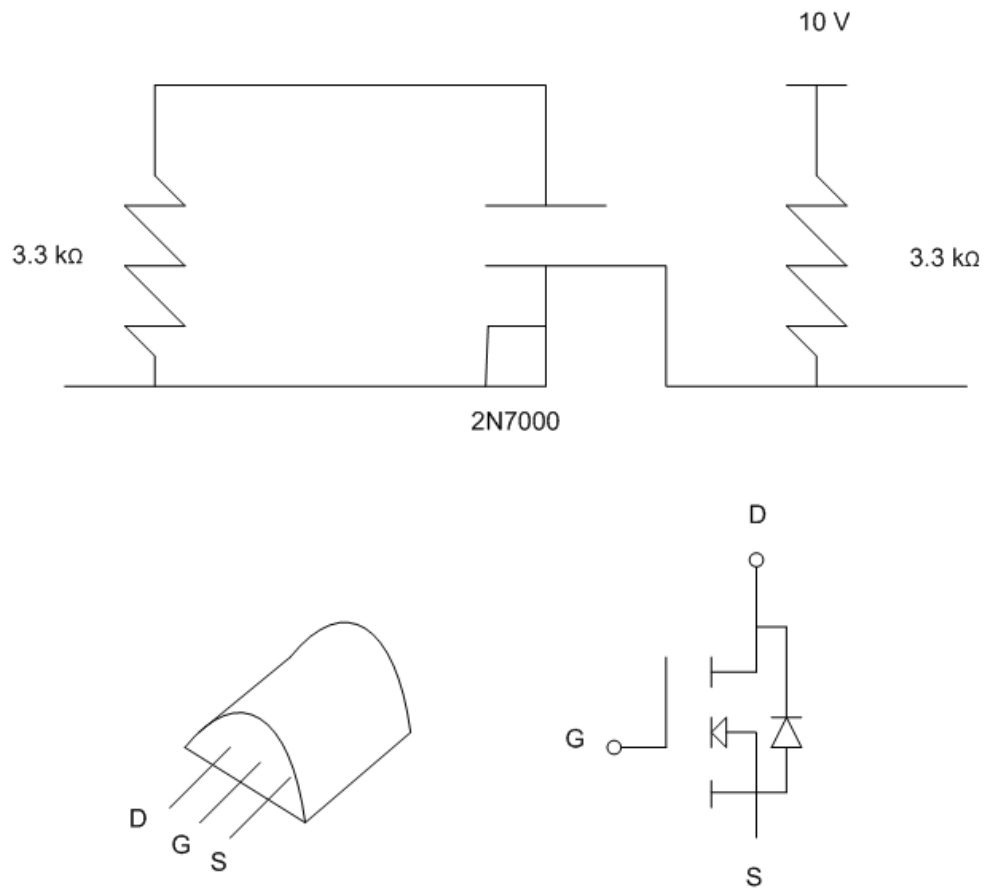


Figure 4.3: Trigger circuit

4.5 Experimental Protocol

In order to study balance, we decided to observe first the natural sway and then the response to an internal, voluntary perturbation: an oscillation.

To enhance repeatability of the experiment we developed a test protocol for the two kinds of test. The subjects had to stare at a point placed in front of them at around the eyes height, and the room in which the test took place was extremely quiet with very low sounds.

Natural sway

The subject was told to stand in the Romberg position on the force plate. To help him, a mask with the correct position of foot was placed on the first force plate. The test lasted 60 seconds, but the interval taken into account was 30 seconds as suggested in literature, since the first and the last 15 seconds need to be eliminated because of the ‘setting time’ and ‘unloading time’. For some test we asked the subject to activate the entire muscle complex.

Auto-oscillating perturbations

The subject was told to stand in the Romberg position on the force plate. In this case the subject had to oscillate in the sagittal plane, with the foot perfectly grounded to the floor and with no movement of the heels. The duration was the same for both tests.

In the order to not fatigue the subject the test were performed with 30 seconds of rest between one trial and another.

Chapter 5

Model validation: Identification methods and simulation

5.1 Identification

System identification is a methodology for building mathematical models of dynamic systems using measurements of system inputs and outputs.

Usually system identification uses the black box model, to relate the inputs and the outputs. This means that the data are fitted without regarding a particular mathematical structure of the model (24). Other possible approaches are grey box models or analytical models.

In this work we consider a time invariant linear system: the response of the system does not depend on absolute time, the response to a linear combination of the inputs is a linear combination of the system to a linear combination of the response to single inputs. Due to the digitalization of measurement we can apply a discrete time model.

Greybox model estimation

In this situation we hypothesize the model structure from physical principles. This is the greybox model estimation, where it is possible to specify the structure of the model with a set of differential equations(42). We modeled the ankle complex as a mass-spring-damper angular system, as seen in section 3.8 the general equation for this linear single degree of freedom system is;

$$m\ddot{\theta}(t) + c\dot{\theta}(t) + k\theta(t) = u(t) \quad (5.1)$$

Where
 m is the mass of the system;

c is the damper coefficient;
 k is the spring stiffness;
 $\theta, \dot{\theta}, \ddot{\theta}$ are angular displacement, velocity and acceleration.

For the discrete system

$$\begin{aligned} t_i &= (i-1)\Delta t \\ \dot{\theta}(t_i) &= \frac{\theta(t_i) - \theta(t_i - \Delta t)}{\Delta t} \\ \ddot{\theta}(t_i) &= \frac{\theta(t_i + \Delta t) - 2\theta(t_i) + \theta(t_i - \Delta t)}{\Delta t^2} \\ u(t) &= u_{(i-1)} \end{aligned} \quad (5.2)$$

we apply the substitution:

$$\begin{aligned} \theta_{i+\Delta t} &= \theta_i \\ \theta_i &= \theta_{i-1} \\ \theta_{i-\Delta t} &= \theta_{i-2} \end{aligned} \quad (5.3)$$

$$\begin{aligned} \dot{\theta}_i &= \frac{\theta_{i-1} - \theta_{i-2}}{\Delta t} \\ \ddot{\theta}_i &= \frac{\theta_i - 2\theta_{i-1} + \theta_{i-2}}{\Delta t^2} \end{aligned} \quad (5.4)$$

Substituting 5.4 in 5.1

$$\begin{aligned} m \frac{\theta_i - 2\theta_{i-1} + \theta_{i-2}}{\Delta t^2} + c \frac{\theta_{i-1} - \theta_{i-2}}{\Delta t} + k\theta_{i-1} &= u_{i-1} \\ \frac{m}{\Delta t^2}\theta_i - 2\frac{m}{\Delta t^2}\theta_{i-1} + \frac{m}{\Delta t^2}\theta_{i-2} + \frac{c}{\Delta t}\theta_{i-1} - \frac{c}{\Delta t}\theta_{i-2} + k\theta_{i-1} &= u_{i-1} \\ \theta_i \left(\frac{m}{\Delta t^2}\right) + \theta_{i-1} \left(-2\frac{m}{\Delta t^2} + \frac{c}{\Delta t} + k\right) + \theta_{i-2} \left(\frac{m}{\Delta t^2} - \frac{c}{\Delta t}\right) &= u_{i-1} \end{aligned} \quad (5.5)$$

$$\theta_i = u_{i-1} \frac{\Delta t^2}{m} + \theta_{i-1} \left(+2 + c \frac{\Delta t}{m} + k \frac{\Delta t^2}{m}\right) + \theta_{i-2} \left(c \frac{\Delta t}{m} - 1\right) \quad (5.6)$$

This equation ties the experimental data concerning with the angular movement with the sample of the external forces, based on the parameters of the model.

5.2 ARMA model

The Auto-Regressive Moving Average (ARMA) models a combination of AR and a MA models. The AR part involves regressing the variable on its own past values, the MA part involves modeling the error term as a linear combination of error terms occurring contemporaneously and at various times in the past.(ETH)

$$\theta(t) + \sum_{i=1}^{n_a} a_i \cdot \theta(t - i) = w(t) + \sum_{i=1}^{n_c} c_i \cdot w(t - i) \quad (5.7)$$

Where:

n_a is the AR order;

n_c is the MA order;

a_i are the AR coefficients;

c_i are the MA coefficients;

$w(t)$ is the noise;

ARMA models can be solved in Matlab by using the System Identification Toolbox. This toolbox enables the setting of different ARMA models and solution parameters, then it provides tools for solution, visualization and validation, such as residual analysis. A polynomial model is defined by setting its order and when a second order is selected the solution is given in the form:

$$-a_1x - a_2 = y(t) \quad (5.8)$$

The formulas to obtain the dynamic parameters are:

$$c = (1 - a_2) \frac{m}{\Delta t} \quad (5.9)$$

$$k = \left(2 - a_1 - c \frac{\Delta t}{m}\right) \frac{m}{\Delta t} \quad (5.10)$$

5.3 Identification algorithm

To identify the mechanical parameters we wanted to apply to the model we tried different methods: the bilinear regression and the ARMA model in the Matlab System Identification Toolbox.(48)

The input of the two identification methods are the momentum and the angle in the first case, and only the momentum for ARMA model.(SYS)

5.3 Identification algorithm

To obtain the value of the moment it is necessary to define some quantities. First of all the distance of the mass from the center of rotation of the ankle. We used formula 3.1 to calculate the position of the center of mass, while the position and the amount of mass of each segment were taken from anthropometric tables then we took the mean value in time to have a scalar value.

The ankle angle and its velocity were measured as shown in 3.

We consider the rest angle θ_r as the mean of ankle angle, then we use the measured data to create some oscillations around the rest X position of the COM (x_C) and the COP (x_F) X positions. With these oscillation we obtained a new ankle angle and its velocity (7).

$$\theta = -x_C/d;$$

Momentum has been calculated with three different methods:

First method $M = m \cdot g \cdot x_F$

Where m is the total mass;

g is acceleration of gravity;

x_F is the arm and it is the distance from the center of rotation of the ankle and the center of pressure of the foot.

Second method $M = mg \cdot x_F$

Where mg is the vertical component of force;

x_F is the arm and it is the distance from the center of rotation of the ankle and the center of pressure of the foot.

Third method $M = mg \cdot x_C$

Where mg is the vertical component of force;

x_C is the distance from the center of rotation of the ankle and the projection on the x axis of the center of mass.

then we applied the bilinear regression, two subjects, 3 trials each, with the momentum calculated with all these three methods. Matlab Identification Toolbox has been set as a polynomial model, of order [2,2], because we don't have a moment input. The variables result have been calculated as in formula 5.9 and 5.10.

Results are shown in table 5.1, 5.2, 5.3.

5.3 Identification algorithm

			subj1_1	subj1_2	subj1_3	subj2_1	subj2_2	subj2_3
I method	Mk0	Nm	521,23	536,75	511,91	518,04	529,54	506,31
	Mk	Nm	-6,20	0,37	-4,42	2,55	3,71	8,94
	Mc	Nm/s	-85,01	-66,93	-92,17	-86,72	-75,80	-98,73
	Mz		0,00	0,00	0,00	0,00	0,00	0,00
II method	M1k0	Nm	519,61	535,23	508,82	517,24	528,30	501,12
	M1k	Nm	-6,32	0,15	-4,82	2,41	3,48	9,39
	M1c	Nm/s	-86,63	-68,45	-95,26	-87,52	-77,04	-103,92
	M1z		0,00	0,00	0,00	0,00	0,00	0,00
III method	M2k0	Nm	604,63	602,16	601,05	603,94	604,08	599,91
	M2k	Nm	-0,12	-0,21	-0,39	-0,15	-0,22	0,43
	M2c	Nm/s	-1,61	-1,52	-3,02	-0,82	-1,25	-5,13
	M2z		0,00	0,00	0,00	0,00	0,00	0,00
ARMA	K	Nm	603,00	604,63	604,54	621,30	615,51	616,50
	k	Nm	-3,24	0,95	0,46	16,55	10,18	11,46
	c	Nm/s	1234,72	1132,54	998,67	1215,83	1243,45	939,26
	z		0,00	76,36	96,40	19,59	25,51	18,16

Table 5.1: Sway results

We can say that in sway trials the values of k are stable and physically acceptable. As regards damping, only few values are reliable, evidencing a weakness and scarce robustness of procedure. In fact different trials for same subjects present variable values.

Third method is more reliable because the quantities are uncoupled.

For moment calculation seems to be that for auto oscillation we have obtained a good repeatability and reproducibility for the subject's mechanical parameters and values from different subject present rather small variations. So we proceeded with the simulation of auto-oscillations only.

5.3 Identification algorithm

		1_ASC_EO.mat	1_ASC_EC.mat	2_ASC_EO.mat	2_ASC_EC.mat
Mk0	Nm	859,56	860,21	1684,95	318,21
Mk	Nm	312,16	113,27	938,02	-214,38
Mc	Nm/s	-23,90	-157,53	-38,52	-3,22
Mz		-0,10	-0,87	-0,07	0,00
M1k0	Nm	851,40	574,89	1029,66	307,09
M1k	Nm	304,00	-172,05	282,73	-225,49
M1c	Nm/s	-23,63	-107,03	-21,44	-3,46
M1z		-0,10	0,00	-0,08	0,00
M2k0	Nm	544,68	735,33	743,00	-84,50
M2k	Nm	-2,72	-11,61	-3,94	-617,08
M2c	Nm/s	4,95	19,36	13,91	-0,92
M2z		0,00	0,00	0,00	0,00
K	Nm	569,25	876,99	887,01	1197,00
k	Nm	21,86	130,06	140,08	664,41
c	Nm/s	3,11	9,90	4,84	469,98
z		0,78	0,63	0,85	0,04
		4_ASC_EC.mat	4_ASC_EO.mat	5_ASC_EC.mat	5_ASC_EO.mat
Mk0	Nm	1263,50	1107,10	1056,87	699,10
Mk	Nm	730,91	390,97	457,38	99,62
Mc	Nm/s	-12,30	-9,51	-8,51	-2,41
Mz		-0,03	-0,03	-0,03	-0,02
M1k0	Nm	0,00	1130,37	1074,91	710,96
M1k	Nm	-532,58	414,24	475,42	111,47
M1c	Nm/s	0,00	-9,85	-8,64	-2,48
M1z		0,00	-0,03	-0,03	-0,02
M2k0	Nm	0,00	734,02	464,88	441,99
M2k	Nm	-532,58	17,89	-134,61	-157,49
M2c	Nm/s	0,00	4,95	0,93	0,14
M2z		0,00	0,07	0,00	0,00
K	Nm	552,72	727,80	1300,35	1711,15
k	Nm	20,13	11,67	700,86	1111,66
c	Nm/s	3,54	1260,52	863,53	728,35
z		0,74	0,66	0,72	0,99

Table 5.2: Autosway results

5.4 Simulation

		6_ASC_EC.mat	6_ASC_EO.mat	7_ASC_EC.mat	7_ASC_EO.mat
Mk0	Nm	1506,44	1451,01	2370,68	
Mk	Nm	802,96	747,54	1597,16	
Mc	Nm/s	9,42	17,12	26,40	
Mz		0,02	0,04	0,04	
M1k0	Nm	1501,08	1443,53	2349,59	
M1k	Nm	797,60	740,06	1576,07	
M1c	Nm/s	9,61	17,62	26,37	
M1z		0,02	0,04	0,04	
M2k0	Nm	708,41	708,10	776,86	452,27
M2k	Nm	4,94	4,63	3,34	-321,25
M2c	Nm/s	5,65	1,99	5,71	0,10
M2z		0,15	0,05	0,18	0,00
K	Nm	712,43	708,67	776,57	1851,69
k	Nm	8,96	5,19	3,06	1078,17
c	Nm/s	8,49	4,36	12,31	797,03
z		0,17	0,11	0,41	1,40
		8_ASC_EC.mat	8_ASC_EO.mat	9_ASC_EC.mat	9_ASC_EO.mat
Mk0	Nm	1704,13	2142,27	672,10	52,05
Mk	Nm	948,76	1386,90	1,09	-618,95
Mc	Nm/s	1,52	8,99	-0,48	-0,69
Mz		0,00	0,01	-0,03	0,00
M1k0	Nm	1698,48	2140,96	678,57	52,98
M1k	Nm	943,11	1385,59	7,56	-618,02
M1c	Nm/s	2,93	9,33	-0,44	-0,82
M1z		0,01	0,01	-0,01	0,00
M2k0	Nm	760,39	767,06	598,40	672,88
M2k	Nm	5,02	11,69	-72,61	1,88
M2c	Nm/s	4,15	6,75	0,24	2,38
M2z		0,11	0,11	0,00	0,11
K	Nm	841,59	762,64	2104,57	676,41
k	Nm	86,22	7,27	1433,56	5,41
c	Nm/s	1319,29	9,21	977,62	3,74
z		0,65	0,71	0,80	0,10

Table 5.3: Autosway results 2

5.4 Simulation

To validate our results we wanted to use the parameters we just found to activate a model and simulate the output. We needed an input signal to generate the

oscillations so we used a second set of experimental data to obtain the characteristics of the oscillations.

Through a Fourier analysis we identified for each trial the fundamental amplitude, frequency and phase, then we simulated a synthetic oscillation considering a single pure tone with proper amplitude frequency and phase, as presented in figure 5.1. Such synthetic stimulus was applied to the model as an input in order to obtain kinematics from the model. Finally model kinematics has been compared to the measured experimental subject's kinematics 5.2.

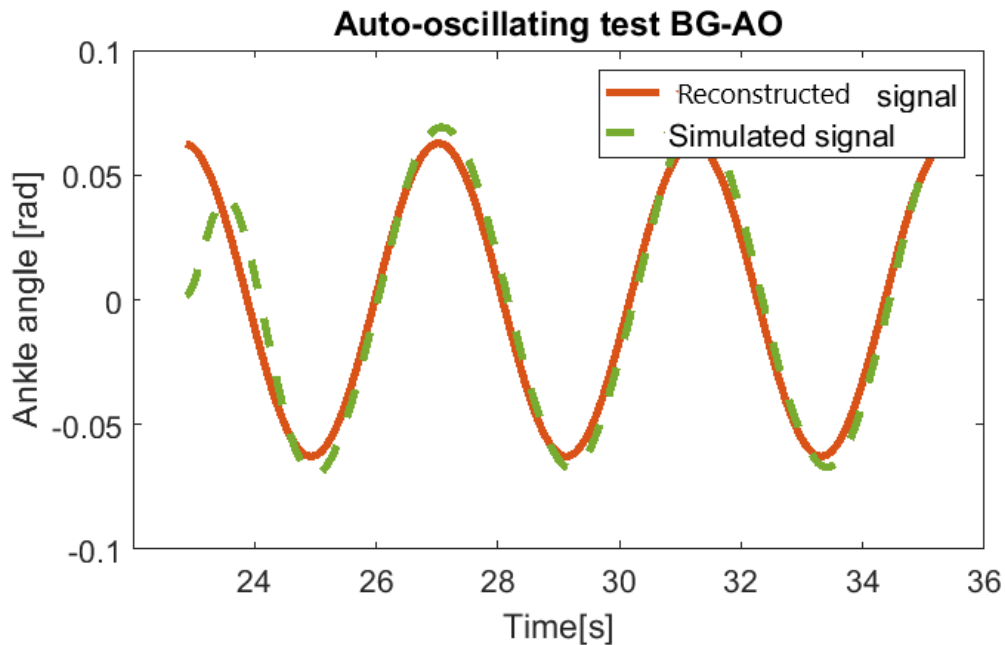


Figure 5.1: Reconstruction of auto-oscillating signal

5.5 Results

In the model set up we have used the parameters obtained by the two identification methods. Results are comparable, but ARMA method demonstrated to be more robust giving stable and repeatable results.

Figure 5.1 presents body angle for an auto-oscillation test and the single tone reconstruction. The correspondence is very good: of course the real signal presents some period variation, that cannot be modeled by a single tone. This synthetic reconstructed signal is then fed to the model, once its parameters have been identified.

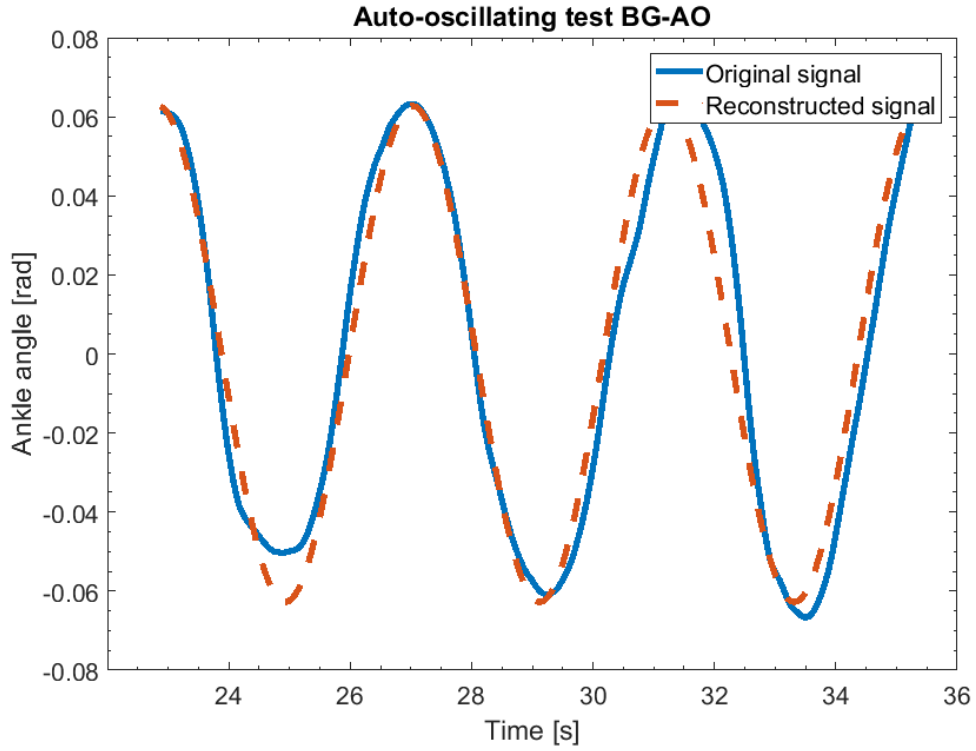


Figure 5.2: Simulation of auto-oscillating signal

Figure 5.2 presents motion angle obtained by the model compared to the reconstructed signal. After an initial transient, their behaviour is very similar, confirming the validity of the proposed approach.

Chapter 6

Model development: Dynamic balance

Methods previously illustrated have been applied to different gestures, characterised by dynamic balance conditions. Gestures have been addressed under different aspects respect to their peculiarity, but they share a focus on dynamic balance.

6.1 Ankle rotation

As a first approach we analyzed the stability of posture using a single degree of freedom on the ankle. We have assumed that the foot is a rigid body while it remains bounded to the floor during sway, but foot and ankle complex contain 26 bones and 33 joints. We believe that it is necessary to split the foot in more than one segment, to better understand the dynamic of locomotion (44).

From a mechanical point of view, considering the Inverse dynamic process, the foot is the first segment who transmit the overall ground force to the leg, so the dissertation about the model of the foot is fundamental.(10)

Measurements and model

To investigate the foot behaviour it is necessary to focus on a simple gesture very controllable and repeatable. For this reason we started this study considering the lift on tiptoes, that can be executed at different heights and velocities simulating what happens during jumping or walking (6). The trials were made in the hospital 'La Colletta' with the measurement system described in chapter 4.

The markers set was composed of six markers placed as described in table 6.1.

Number	Anatomical Landmark
1	Malleolus
2	Heel
3	Metatarsum
4	Top
5	Big toe
6	Small toe

Table 6.1: Foot marker set

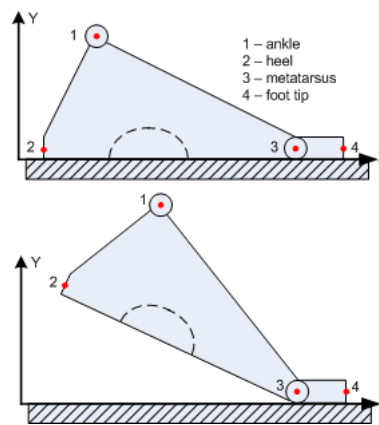


Figure 6.1: Foot model

Position and force data were sampled at 100 Hz. As for the sway analysis, the gesture develop in the sagittal plane, so the model is still planar. The force is applied between the heel and the big toe, as we seen for static balance the center of pressure lays between the malleolus and the foot tip So we can imagine different ways to measure the ankle moment.

Ankle moment measurement

The GRF moment is produced by the force times the lever between the point of application and the ankle joint. These data can be measured as time varying quantities or considered constant or even supposed from the physics of the systems without involving measurements, obtaining different levels of complexity. Firstly, let's consider a static approach: subjects stand in a rest position.

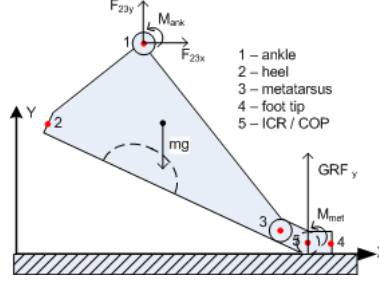


Figure 6.2: Forces acting on foot

$$M_s = mg \cdot (\hat{X}_{met} - \hat{X}_{mal}) \quad (6.1)$$

Where

m is the subject's mass;

g is the acceleration of gravity;

$(\hat{X}_{met} - \hat{X}_{mal})$ is the lever in the hypothesis that the weight is fully applied in a point with the same metatarsus X coordinate;

Where the hat superscript represents a measured quantity.

In the case of a dynamic gesture in which the subject's weight is not a good approximation of force, and the application point of the force is in motion we need to measure the force acting on foot segment.

For this reason we measured the force and two different approach are proposed:

$$\begin{aligned} M_1 &= \hat{F}_y \cdot (\hat{X}_{met} - \hat{X}_{mal}) \\ M_2 &= \hat{F}_y \cdot (\hat{X}_{COP} - \hat{X}_{mal}) \end{aligned} \quad (6.2)$$

These two equations differs in the definition of the lever: in the first case the point of application of the force is the metatarsum, in the second it is the COP. Measuring force it is possible to consider the horizontal contribution of the force:

$$\begin{aligned} M_{1xy} &= \hat{F}_y \cdot (\hat{X}_{met} - \hat{X}_{mal}) + \hat{F}_x \cdot \hat{Y}_{mal} \\ M_{2xy} &= \hat{F}_y \cdot (\hat{X}_{COP} - \hat{X}_{mal}) + \hat{F}_x \cdot \hat{Y}_{mal} \end{aligned} \quad (6.3)$$

A common hypothesis is such approaches is that the entire foot acts as a rigid body and it can be modeled by a single segment during the gesture considered. In this case, during the contact with the ground, the foot rotates around the GRF point of application. Let us consider gesture like a jump or lifting on foot tips: in this case the foot may be modelled by two segments, from malleolus to a point along foot sole the metatarsus, and from metatarsus to the foot tip. In

such cases the rotation of the proximal part of the foot is around an ideal point called instantaneous centre of rotation, ICR (5). The position of such a point can be measured considering the velocities of different points on the rotating body considered rigid. So the equivalent ankle moment can be measured considering the external force applied in the ICR, as in the following:

$$M_3 = \hat{F}_y \cdot (X_{ICR} - X_{mal}) \quad (6.4)$$

A further alternative is a different foot model in which foot is split in two rigid sections, and the ankle moment is obtained through the solution of the dynamic equations:

$$M_4 = M_{ank} = J_1 \ddot{\theta}_1 + F_{12y} \cdot (X_{met} - X_{mal}) - F_{12x} \cdot (Y_{met} - Y_{mal}) + mg \cdot X_{COM1} \cdot \cos(\theta_1) + M_{met} \quad (6.5)$$

Where M_{ank} , M_{met} are torques measured at the ankle and metatarsum according to the biomechanical model; J_1 is the foot inertia; θ_1 , $\ddot{\theta}_1$ are foot angle and angular acceleration; F_{12x} , F_{12y} are force components between the two foot segments.

Experimental results

In figure 6.3 it is shown that the vertical component of the GRF is far larger than the horizontal one. Figure 6.4 shows a metatarsus almost stable in a static position, at the same time, it is clear that the GRF application point is moving from middle foot sole, toward foot tip, as shown by the black line. The ICR of the foot part lifting on the tip is presented in blue and it follows the same COP behavior, confirming that the rotation is about the point of application of the external force. Noise on the ICR signal is due to the processing required to evaluate its position.

Measurement data presented in figure 6.4 are the model inputs for ankle moment measurements following the approaches presented in section 6.1.

The difference from the first method M_s and the second M_1 is due to the GRF time behaviour, in M_2 the COP in measurement of the lever is introduced, and this difference underlines that the metatarsal approximation isn't valid in this case. M_3 based on ICR shows a behaviour similar to M_2 suggesting that in this case COP is a good approximation of the point around which foot rotation takes place.(9)

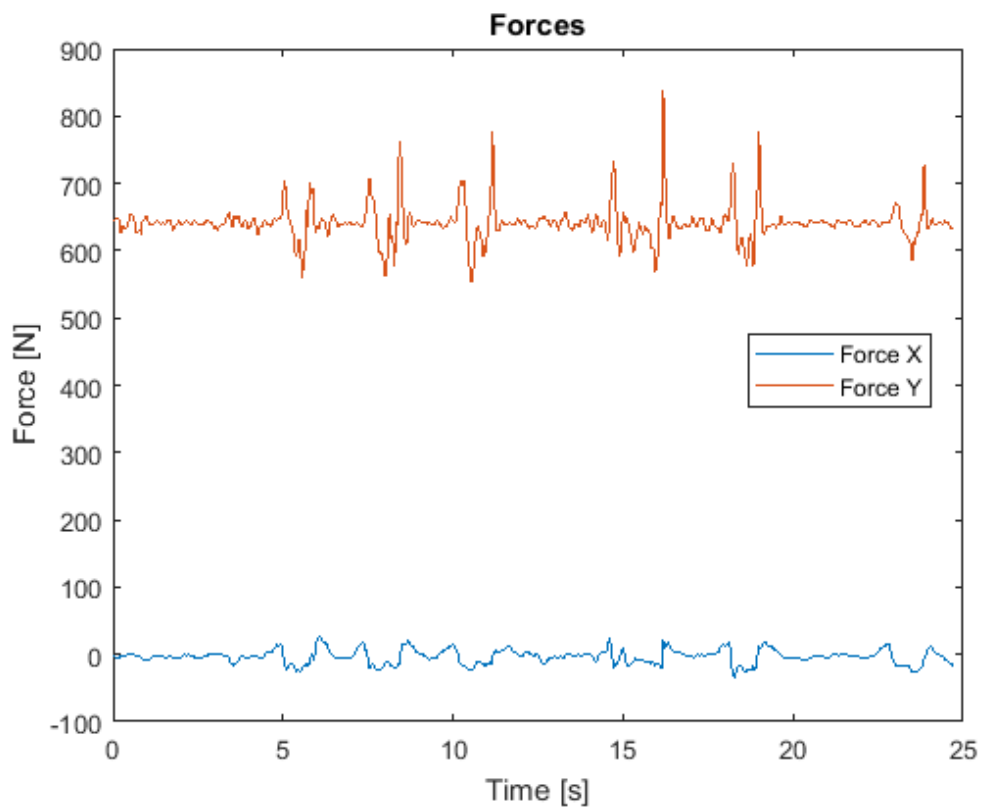


Figure 6.3: GRF components in vertical (Y) and anterior-posterior (X) direction

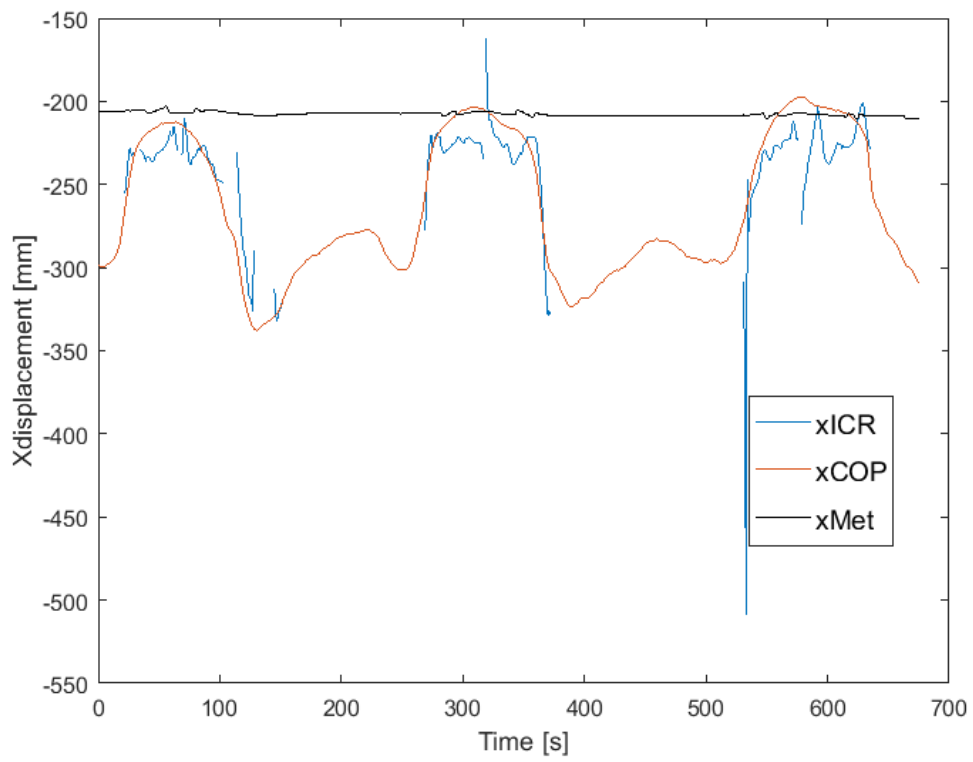


Figure 6.4: Metatarsum, COP and ICR

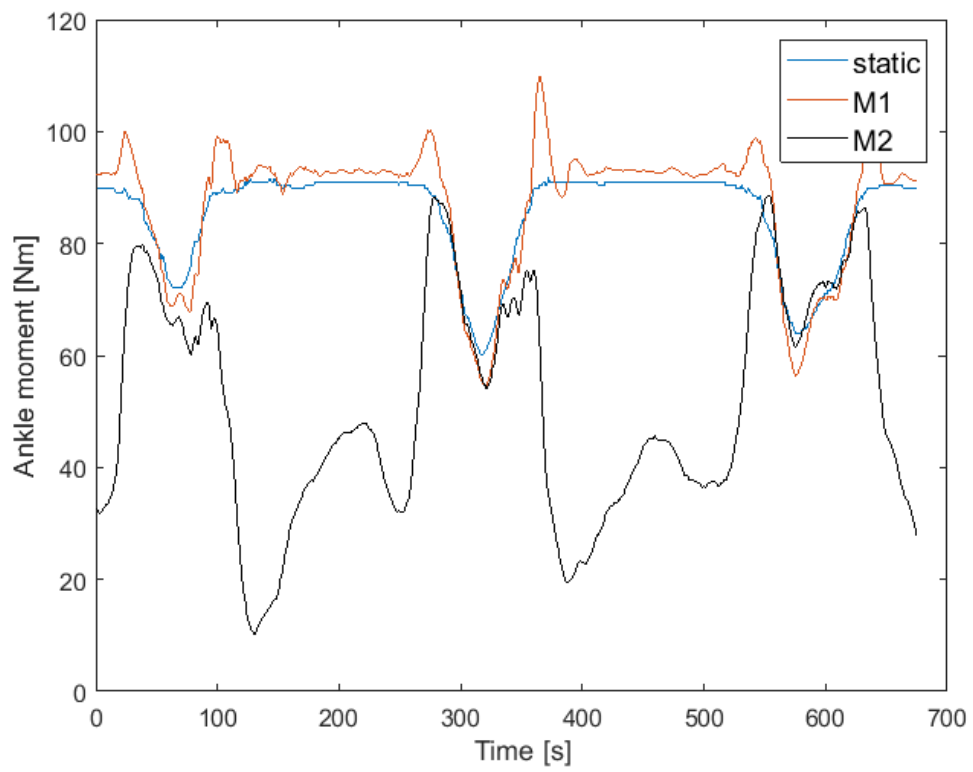


Figure 6.5: Ankle moments measured according to different approaches

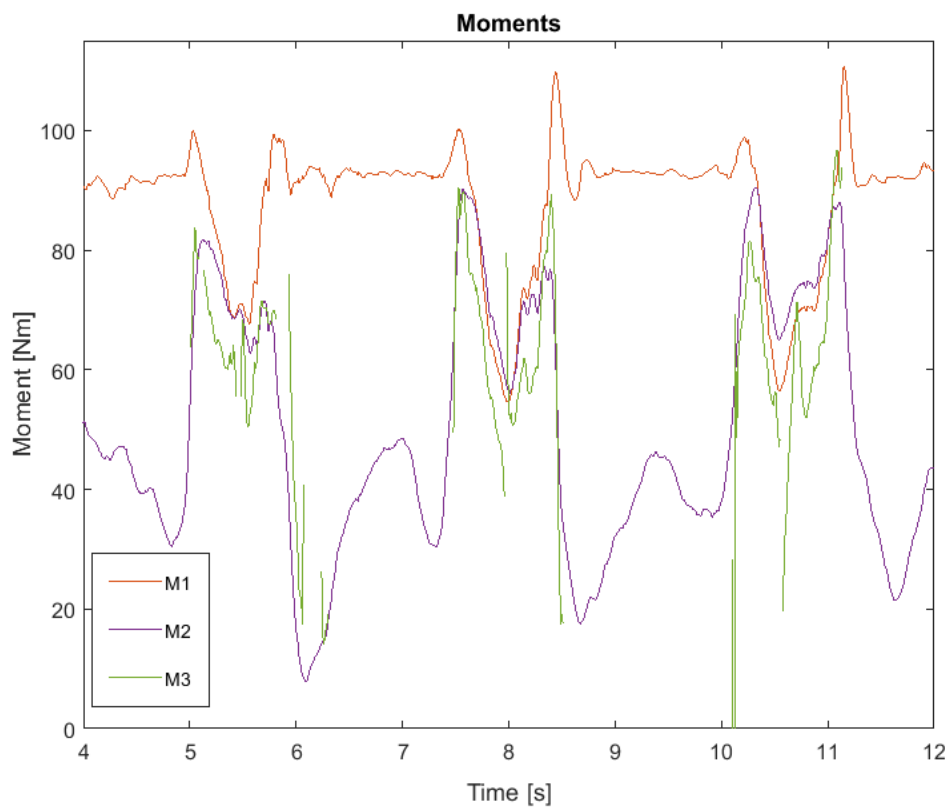


Figure 6.6: Ankle moments measured according to different approaches

6.2 Weight Lifting

Another gesture in which the foot, its position and sustain is very important is weight lifting.

In weight lifting the control of posture is fundamental to prevent injuries in athletes who mainly lament pain on articulations (12). There are not many studies who compare different point of application of force during lifting in a quantitative way, although athletic trainers give precise instructions how to manage foot posture: on heels, the tip and the center of the foot.

The fundamental and primary posture to learn in weight lifting is the *Squat lifting*(46). It consists in two phases: crouching and lifting. The movement starts standing with knees extended, then the subject crouches and flexs the trunk till he reaches the position in which the centers of rotation of knee and hip, are aligned and the femur is parallel to the ground (33). This position is called the 'bottom position', then the subject lifts up. To facilitate the execution a kind of specific technical shoes have been studied on purpose: the sole is very flat and stiff, with a heel of about 20 mm (15). Main aim of these shoes is to stabilize the foot under the load, secondary the wedge improve the position of the COP under the footsole.

The protocol designed for this gesture comprehend some trial without shoes to confront the effect of shoes on the COP, the ground reaction forces and the posture during the same gesture with different loads (32).

Measurements and model

The experimental set up we are using is a couple of force plates BTS P6000 and a camera Dalsa Falcon (4.1), for this gesture it is indicated to place feet on each force plate, in order to caught the behaviour of the COP under each foot and the possible unbalance in weight distribution.

The marker set was composed of 8 markers, placed as shown in table 6.2

The protocol prescribed six kind of trials: posture loading on the metatarsum, on the heel and on the middle foot, each with and without proper shoes. The specific gesture is the 'back squat-high bar' in which the bar is led against the acromion and the scapula, each trial was performed both with a low weight (8 kg) and with a high weight(44 kg).

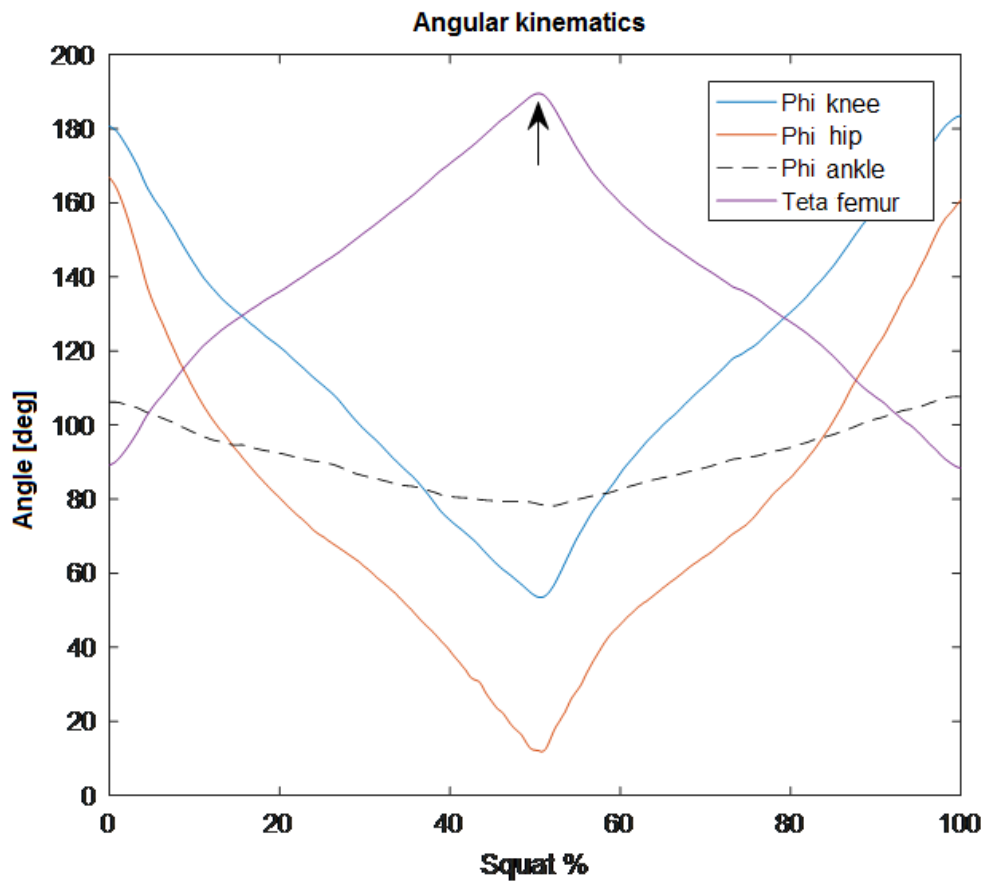


Figure 6.7: Angular kinematics

Number	Anatomical Landmark
1	Malleolus
2	Heel
3	Metatarsum
4	Big toe
5	Knee
6	Hip
7	Iliac crest
8	Shoulder

Table 6.2: Marker set

Experimental results

As seen in figure 6.7 starting position of relative angles is about 180 degrees, reaching a minimum of 60 degrees for knee and 30 degrees for the hip. To produce a posture accepted in agonistics it is necessary that the femur reaches the parallelism with the ground and it is underlined in figure 6.7, with the maximum femur angle major than 180 degrees.

The difference between the ankle angles with or without the shoes is shown in figure 6.8, it is possible to notice that the presence of shoes allows the subject to have a range of motion of this angle higher in the situation with shoes. Probably the presence of the rigid heel moves the center of pressure in a more stable position allowing the athlete to perform the gesture with a higher confidence.

In figure 6.9 it is possible to observe how the COP moves backward in case of the squat with the higher weight, the mean value of the COP for the same subject moves of 40 mm, the 15% of the total length of the foot.

In this case it is necessary to model it with a multisegmental model.

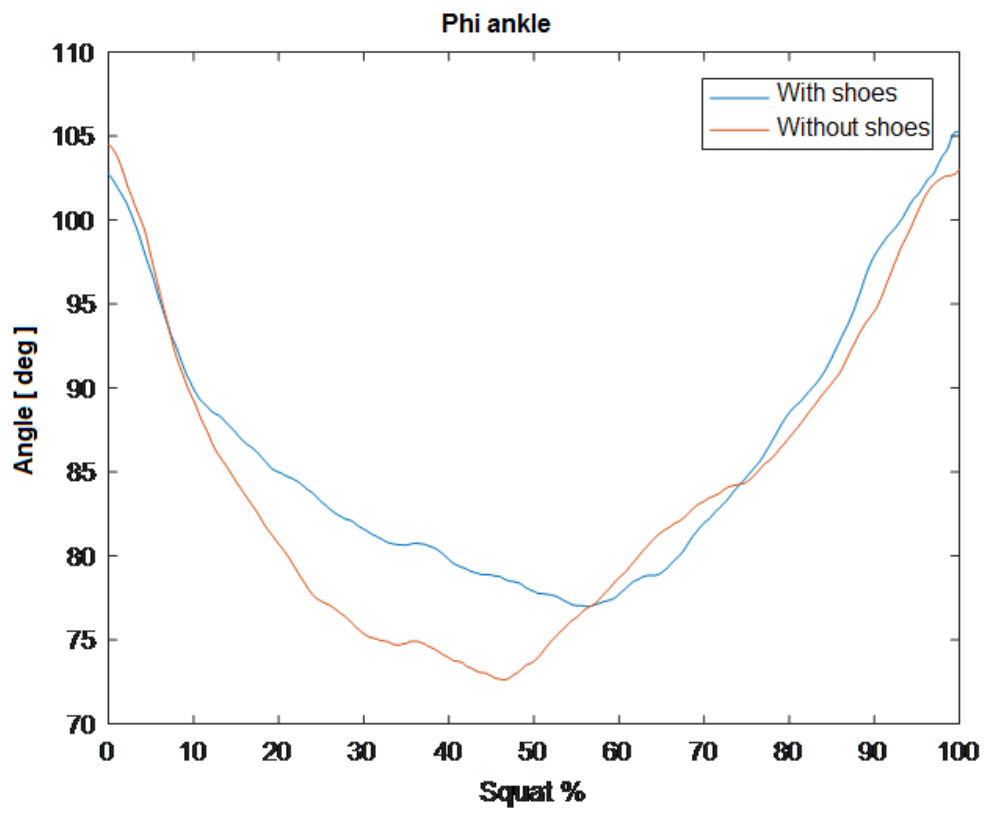


Figure 6.8: Ankle angle comparison with or without shoes

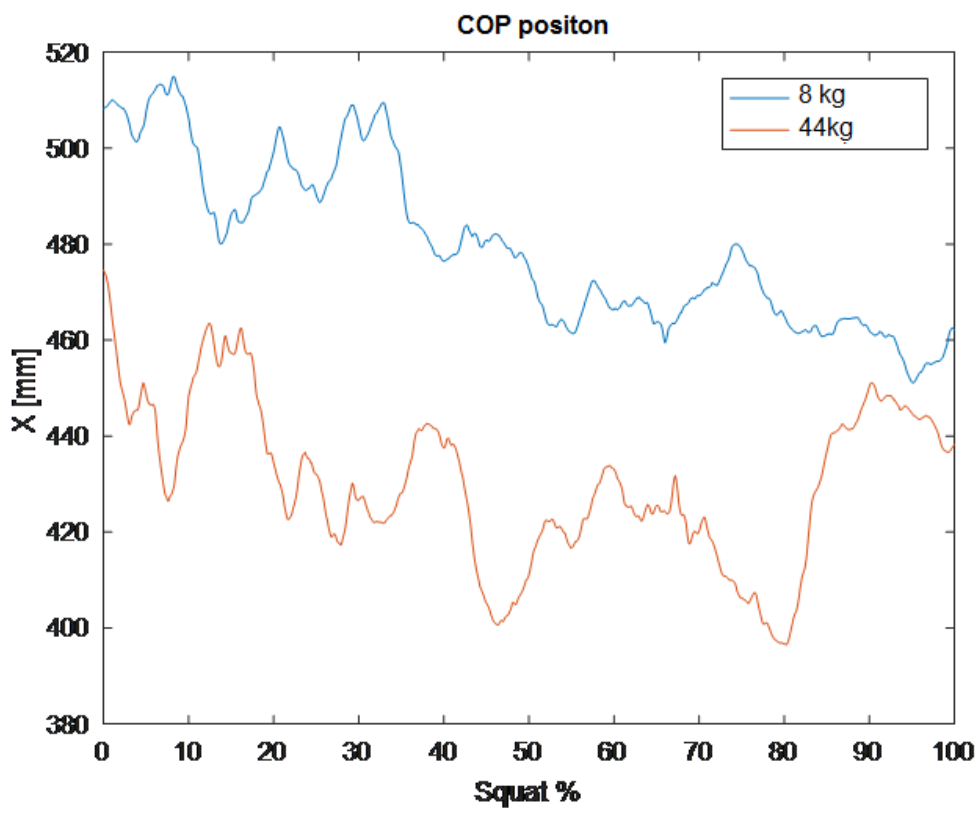


Figure 6.9: Total COP comparison with or without shoes

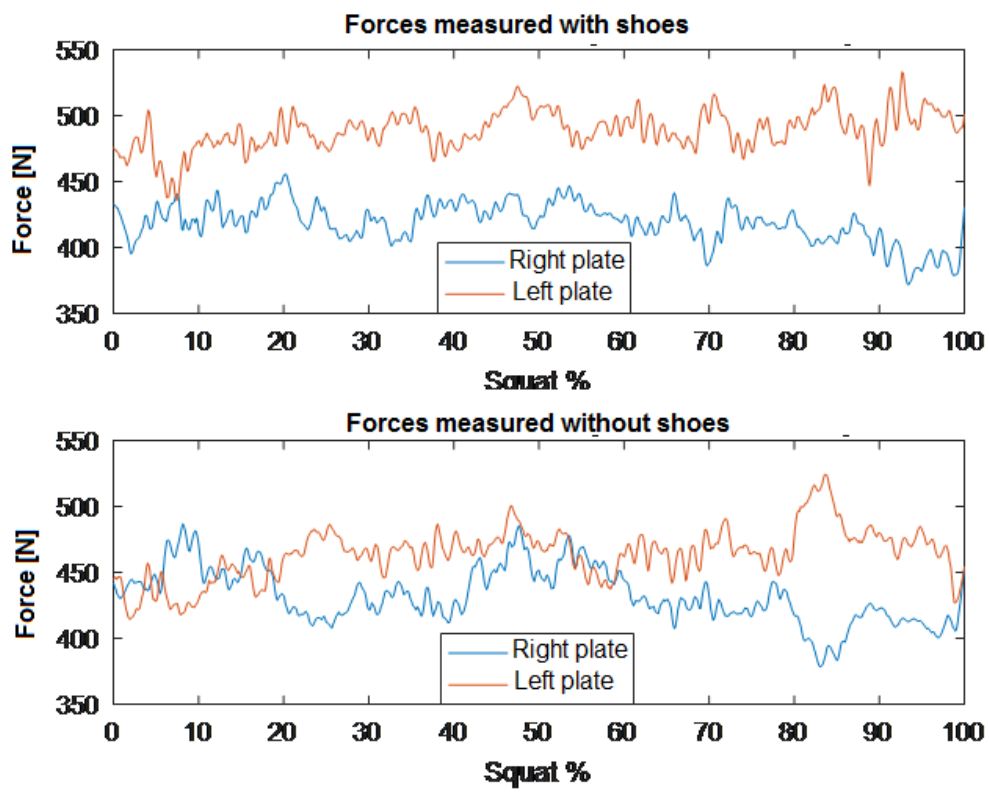


Figure 6.10: Forces comparison with or without shoes

6.3 Squat jump

When a multisegmental model is used, the number of bodies grows with the complexity level we want to investigate, in this case we use a more complex model to make some energetical considerations about movement, in particular in the following we consider the power measurement in maximum height jump (4).

Maximum height jump is frequently used to measure athletic performances, in particular when the focus is on explosive power(23). Sports most involved are volleyball and basketball, sprint, high and long jump (3). Besides that, this kind of test is used to measure the overall training level or improvement in athletic training programs. There is no recognised standardization neither for the test protocol itself, (2) nor for required measurement system and measurement method, and for signal processing (54) (52)

A few jumping techniques may be considered, as well as measurement methods with different complexity and possibly reliability. One possibility is to perform a high jump from a standing position and the measurement of the maximal height the subject is able to reach by extending his arms, in this case performance is evaluated by the differential between the maximum height reached and the height with subject standing on the floor (45).

Comparing test results from different training periods or different subjects a very basic performance evaluation can be carried out, to determine training-period effects or to select athletes in better conditions or most suitable for a specific sport. In this simple case usually the height is measured by the subjects touching a reference scale on the wall with the hand covered by chalk(43). More sophisticated measurement systems include video recording, throw wire encoders and similar devices.

Moreover, a complete characterisation requires a subject instrumented with proper markers placed on specific anatomical landmarks which displacement is recorded while the subject executes the test on a force platform. Such a system enables a complete characterization of the biomechanical kinetics, by measuring the forces exchange with the ground, and kinematics in two or even three dimensional space, if more than one video camera is used (5). Different test modalities are reported in the literature (29). Traditional squat jump starts from a static position with knee and hip flexed and the jump takes place by a fast whole body elongation including arms(25). Another possibility is a dynamic pre-activation by a counter-movement requiring muscles elongation, followed by a fast contraction. It has been found that such a condition increases power output, probably due to muscle and tendons elastic properties (36). Time history of the measured quantities, such as reaction force or joint angles or even power output can give useful information if correlated with surface electromyography muscle activity measurements. The

repeatability of the measurement is not available because the jump is usually 'One Repetition Maximum' in fact the test protocol allows only one jump, because the muscles lose their complete power in just one jump and the recovery time is long and that means that the psychological conditions of the subjects are not the same after this time. Here is proposed to measure directly the power, this quantity is directly proportional to the performance, instead of the height or the velocity. Power is not easy to measure: here we confront different methods to compare their results and verify their behaviour.

Power measurement

Instantaneous mechanical power output from a jump test is defined as the scalar product. (14)

$$P(t) = \mathbf{F}(t) \cdot \mathbf{v}(t) \quad (6.6)$$

Where

$\mathbf{F}(t)$ is the force applied to the body COM;

$\mathbf{v}(t)$ is its velocity.

Since the gesture develops above all in the vertical direction, we can consider only power contributions from vertical force and velocity. So we can define power output as:

$$P(t) \cong F_y(t) \cdot v_y(t) \quad (6.7)$$

Such power can be measured according to a few methods on the basis of the raw measurement data available. Let's consider the first method based on force data only. The ground reaction force vertical component can be directly measured by the force platform, while vertical CoM velocity can be obtained through the integration of acceleration obtained from the same GRF data:

$$P(t) \cong (F_y(t) - mg) \cdot \int_0^t \frac{F_y(t') - mg}{m} dt \quad (6.8)$$

Where

$F_y(t)$ is the vertical force component as measured by the force platform;

m is the subject's mass;

g is the gravity.

Note that we have considered only the dynamic contribution to GRF, by subtracting the force due to subject's weight. Of course if we can measure the CoM vertical velocity a mixed method might be considered. In this case we have two possibilities: approximating the CoM vertical position with the standard

6.3 Squat jump



Figure 6.11: Subject during test

Number	Anatomical Landmark
1	Shoulder
2	Iliac crest (or approximate body CoM)
3	Hip
4	Knee
5	Malleolus
6	Heel
7	Metatarsus
8	Foot tip

Table 6.3: Foot marker set

anatomic position on the iliac crest, or computing the CoM vertical position according to the vertical positions of the CoM of segments constituting the body. In the former case we are considering subject's body as rigid, while in the latter this second case we take into account CoM movements due to the different body configurations during test executions.

$$P_m(t) \cong (F_y(t) - mg) \cdot \dot{y}_{COM}(t) \quad (6.9)$$

Lastly, if we have only kinematic measurements without force platform data, it is possible to obtain CoM acceleration and velocity from position through proper differentiation procedures cite.

$$P_k(t) = m \cdot \ddot{y}_{COM}(t) \cdot \dot{y}_{COM}(t) \quad (6.10)$$

Measurement set up

The experimental set up we are using includes a force platform based on four load cells, a motion capture system based on a set of active markers and a camera, and a personal computer with a data acquisition board and dedicated software as described in 4 Markers are high intensity white led, and are placed on main anatomical landmarks of subject's right side as shown in table 6.3

A video is recorded at maximum frame rate maintaining full camera resolution and no compression. Ground reaction force vertical component is measured by a custom force platform, based of 4 calibrated load cells with an overall measurement range of 10 kN and a bandwidth of approximately 100 Hz. Acquisition

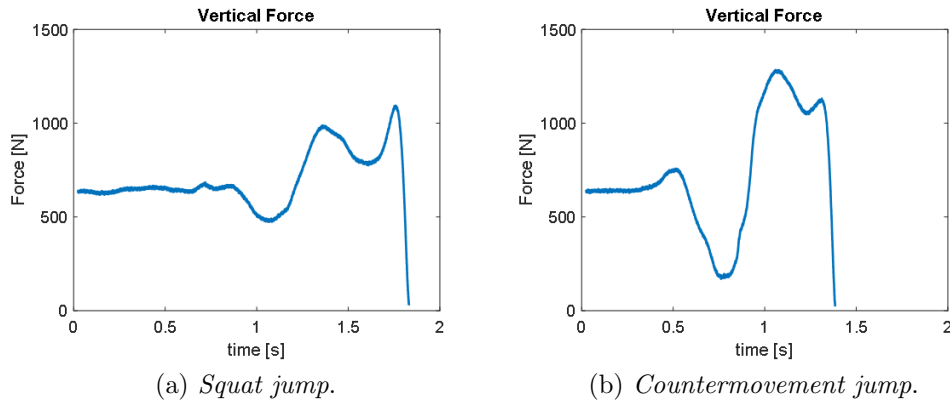


Figure 6.12: Vertical forces in jump

takes place at 5kHz and it is synchronised with the video system.

Results

The test sessions were arranged to have a sequence of four jumps: squat jump, with and without upper limbs contribution; countermovement jump with and without upper limb contribution.

Force time history is presented in figure 6.12, while figure 6.13 presents power output measurements. The three methods present good consistency both in the time history development and in the maximum value. Since a reference method is not available, an energy balance validation procedure could be of help for power measurements metrological characterisation.

Mechanical power is used to increase whole body CoM potential and kinetic energy, power integration should correspond to the potential energy at the maximum of its elevation, as shown in 6.14, due to the initial movement CoM height decreases before jumping, a comparison based on energy variation seems to be more robust.

As shown in 6.16, potential energy variation indicates that most reliable methods are pure kinetic and pure kinematic based on approximated CoM.

Pure methods present a maximum difference on peak power values around 100 W on peaks of 2 kW, depending on jumping method.(8)

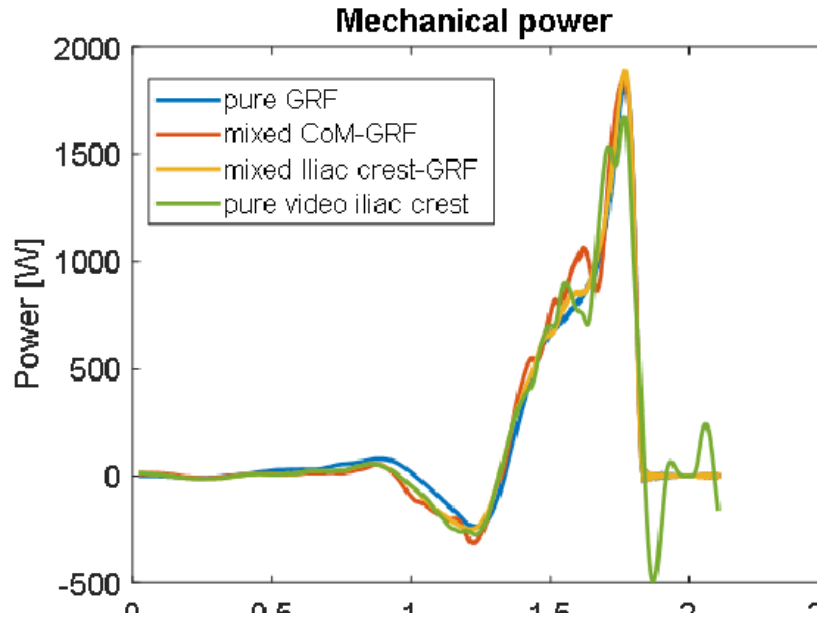


Figure 6.13: Mechanical Power measurement

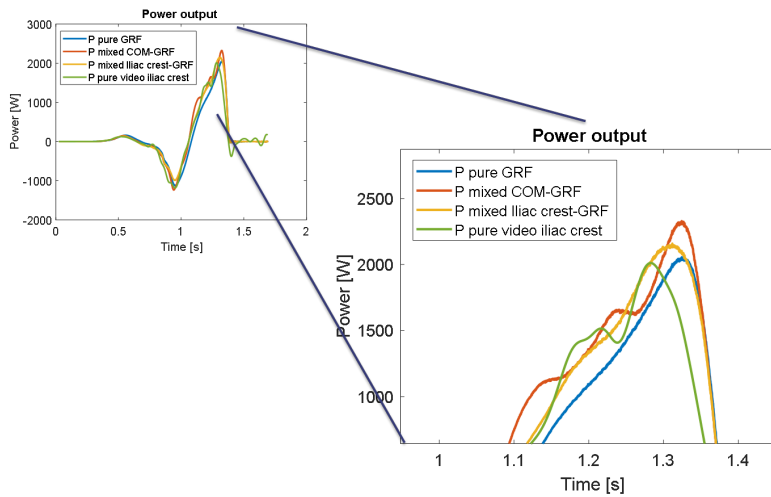


Figure 6.14: Mechanical Power Peak

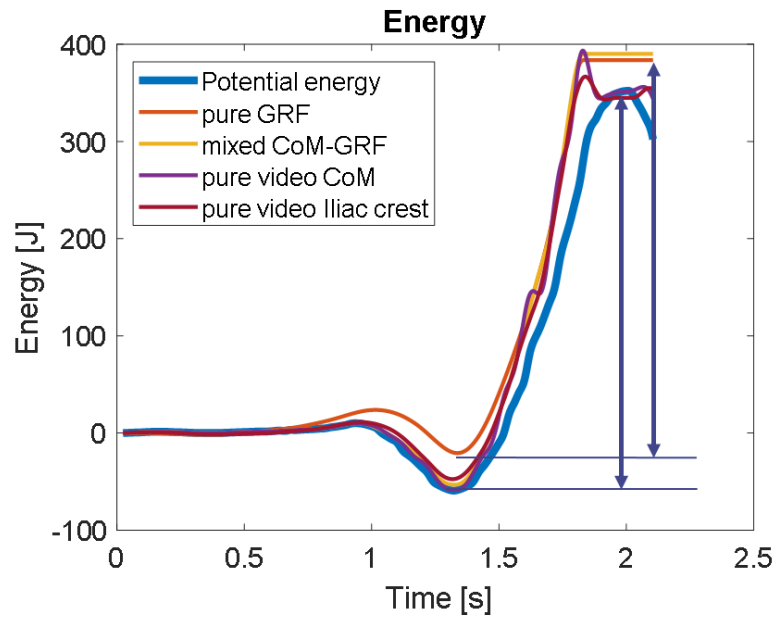


Figure 6.15: Mechanical Energy measurement

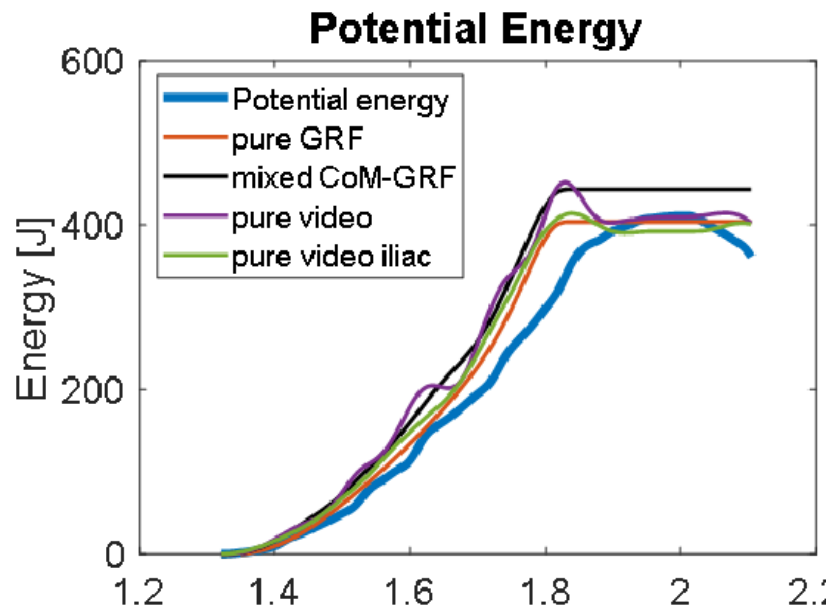


Figure 6.16: Potential Energy measurement

Chapter 7

Conclusions

This work is a contribution to the biomechanical study of human movement, balance mechanics and control. The purpose was to examine in depth some peculiar aspects of balance models in biomechanics in dynamic condition.

The thesis stated the problem of modeling human body from a pure mechanical point of view. The main focus of the work has been to develop a model of human body which could describe the balance method used by humans to maintain balance during standing and during gestures like rotating on foot tip, hopping and jumping.

The main goal we wanted to achieve was a purely mechanical multibody model in which also control characteristics are merged in the two dynamic parameters, stiffness and damping at the joints. We described the dynamic behavior of whole body with mechanisms coincident with the anatomical joints, which describe the control biomechanics of the entire body-joint complex, without entering the details of joints anatomy.

A flexible measurement system has been realized to perform experimental trials for each gesture analyzed, as described in chapter 4, I've dealt with its metrological characterization and validation. My work also included the design, the development and testing of a measurement system and its software to synchronize the measurement instrumentation and to elaborate data with a tracking algorithm for markers, usable in the laboratory with a flexible structure respect to the different sensors and kind of biomechanical gesture analyzed.

In the case of balance the model has been developed and its mechanical characteristic were determined as seen in chapter 3. Then a simulation to validate the model has been performed to define the validity and the limits of application

of such model.

A redesign of the model has been necessary as seen in chapter 6, to study more complex gestures: the inverse pendulum model has been 'broken' in a multisegmental model to better describe the behavior of human body.

A particular focus has been put in the problem of the definition of the instant center of rotation, as seen in chapter 3. To understand the mechanism of moment transfer from the foot to the leg, has been developed the modeling of the foot and the recognition of the position of the Center of Pressure respect to the point of articulation of the foot. The importance of instant center of rotation of the foot has been analyzed. During the study of the jumps, also important collateral themes have been afforded like energetic aspects and power output, with interesting application in sports field 6.

The study provided an overall insight in dynamic balance during different gestures. The attempt to adopt a purely mechanical model has been successful in some cases while some improvements are required in other. As regards sway and response to external small disturbances the system parameter identification has been satisfactory and the validation loop demonstrates that the model is reasonably accurate to describe the bionmechanical situation. Of course the identification procedure is by far the most critical step in model development. As regards this specific point several methods have been tested and the most appropriate, even if not robust enough, according to the data available is the bilinear regression.

Since this study is transversal to different gestures, several biomechanical modeling issues have been afforded. In particular model complexity has been adapted to the gestures, changing for example the number of DoF. An interesting issue emerged regarding the Instantaneous centre of rotation of the foot. Such point is essential if the model included a non rigid single element foot, but a sort of flexible or multibody foot. The location of the ICR enables the evaluation of the moments due to foot fingers on the ground that seems to be important when dealing with hopping or jumping and also in the last contact phase in walking and running.

The instruments and measurement systems developed during this thesis are available in the lab and are actually used to characterise human movement and sports performances. As application examples consider the study on the thermal and biomechanical behaviour during prolonged efforts in trade mill running. Cyclist evaluation at constant power output and variable cadence and other future and under development applications.

As regards results exploitation, besides the scientific publications and congress presentation, I want to mention the two national projects submitted for evaluation (one still waiting for the final result) regarding the exoskeletons evaluation with particular focus on the biomechanics of the interactions with the pilot. An European sub-project submitted for evaluation that regards the internal moments

in the upper limbs when walking with the help of an active exoskeleton.

Remarks and future work

In biomechanics different fields of study are used to investigate, its different aspects required different approaches and different knowledges: medical issues as regards the internal anatomy and behaviour of body, modelling to determine internal force and moments, measurement systems, sensors and signal processing to characterise body motion and external forces. In this thesis I had to apply image elaboration methods, identification of mechanical parameters, time-varying signal spectral analysis, technical aspects tied to measurement hardware.

These aspects are necessary to study a scientific field, who has presented unexpected implications, interesting, but not planned, and they requested a long time to be deepened and cleared with confidence.

The results obtained are a higher knowledge of a problem in some of the aspects it presented, but they have to be deepened in some specific aspects.

From my point of view, future work should focus on a multisegmental model with multiple degree of freedom, of a standing human. The tests performed didn't gave a unique identification of mechanical parameters. The trials have been performed in different laboratories and sometimes results seems not to be compatible. A new protocol for sway tests should be introduced because the natural sway oscillations didn't gave reliable results, and a repeatable external perturbation is required. Main work should deal about the typology of gesture studied and its characterisation.

Other consideration could be taken about the model: in the most sophisticated version I have used, the foot is articulated instead of the traditional models of foot with a rigid body without degrees of freedom.

This model have been studied only focusing on this segment and should be inserted in the complete biomechanical model. At the moment, the hypothesis is that the torque contribution due of the first segment, which represents the fingerfoot, is significant to stabilize the posture during hopping in place.

Finally, measurement aspects could be improved as usually happens with the introduction of new technologies. Expecially I would like to refer to the inertial measurement systems, whose metrologic performances should be verified respect to traditional vision systems. If the performances would be confrontable it is possible to use these sensor in any environment without requiring a gait lab.

Regarding to the video instrumentation aspects the system could be improved under two different aspects: the markers and the tridimensionality. The active markers could be replaced with passive markers, the sistem could be also replaced with systems based on the digital image correlation (DIC) now used on deformation analysis or on little displacements detection.

Appendix A

Simulators

A.1 OpenSim

OpenSim is a freely available software package that enables people to build, exchange, and analyze computer models of the musculoskeletal system and dynamic simulations of movement. It is used in field as biomechanical research, ergonomics, medical device design, robotics, sport science and education. ([OpenSim](#))

There are two possibilities to use this software, the creation of models and the use of models shared with the community by the creators.

Create a new model in OpenSim

The structure of a new model in OpenSim is depicted in the API of OpenSim with an extension to Matlab and Python. A model is a segmental model of rigid bodies connected by joints and acted by forces.

To create a model it is necessary to produce a text file in XML language, the software we used to produce these models is Notepad++. The parts of the models are: bodies, joints, forces, markers, constraints, contact geometries and controllers. ([OpenSimDocumentation](#))

There is a 'ground body' bounded to the ground, other bodies are connected one to another and to the 'ground body' with a joint, the sequence is hierarchical (parent-child) from the 'ground body' descending to further bodies.

Muscles are force elements that acts on bodies with a certain insertion point,

level of activation and length. Others forces in OpenSim are external forces, as reaction forces, passive spring-dampers and linear and torsional actuators. Muscles are most frequently modeled with the Hill model, but for specific applications it is possible to feed the model with a specific behavior, like spasticity.

Use an existent model with an original marker set and experimental data

Scaling tool

For each subject it is necessary to have a photo of marker set up and a static trial. The first step is to scale the model on the dimensions of the subject of the trial, during this process it is possible to let some virtual marker to move on the model to fit better the data of the static trial and it is still possible to manually scale the segment. The algorithm scales joint frame locations, mass center location, force application points, and muscle attachment points. The output of this procedure is a new scaled model.

Inverse kinematics

When the model and the subject fit it is possible to recreate the movement in the model with the 'Inverse Kinematic' procedure. Both of these procedures solve the weighted least square problem to minimize the distance from the marker data position and the virtual marker data position. In the first case the variables are the length of segments and the markers position, while in the second the variables are the joint angles.

The output of this procedure is a set of model postures during time.

Inverse kinematics

When model positions in time are defined and velocities and accelerations are calculated, it is possible to apply the Euler equations of motion and obtain the moment at the articulations.

The outputs of this procedure are the joint moments vs time.

Static Optimization

The Static Optimization Tool uses the known motion of the model to solve the equations of motion for the unknown generalized forces (e.g., joint torques) subject to one muscle activation-to-force condition: omogeneous force distribution between muscles.

The output of this procedure are the muscle activations which cause motion.

Forward dynamics

In contrast to inverse dynamics where the motion of the model was known and we wanted to determine the forces and torques that generated the motion, in forward dynamics, a mathematical model describes how coordinates and their velocities change due to applied forces and torques.(47)

The output of this procedure are the joint angles due to the muscle activations which cause motion.

A.2 Simulink

Simulink ([Simulink](#)) is a block diagram environment for multidomain simulation and Model-Based Design. It supports system-level design, simulation, automatic code generation, and continuous test and verification of embedded systems. Simulink provides a graphical editor, customizable block libraries, and solvers for modeling and simulating dynamic systems. It is integrated with MATLAB.

The model created in simulink uses, as the analytical model and the OpenSim model, rigid bodies connected by joints. The two segment model is linked to the ground and inserted in a physical environment with gravity acceleration.

Data are loaded from protocol trials and through a simulation with an ODE8 solver it is possible to obtain with sensor blocks the value of moment ankle for the inverse problem and the Body COM displacement for the direct problem.

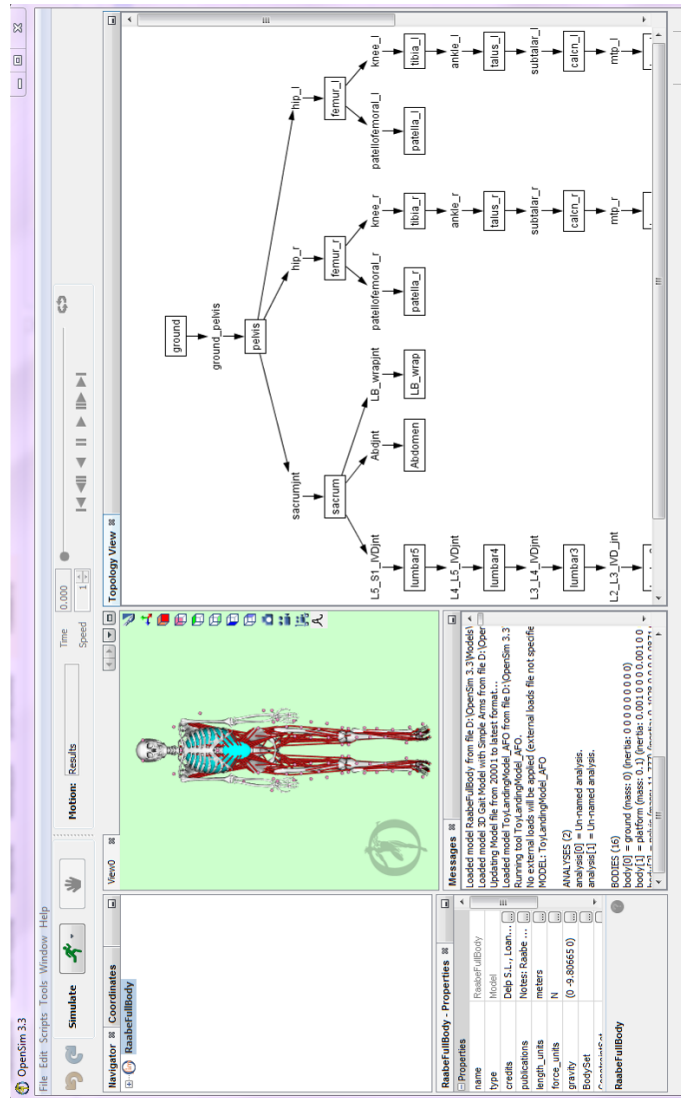


Figure A.1: OpenSim front panel

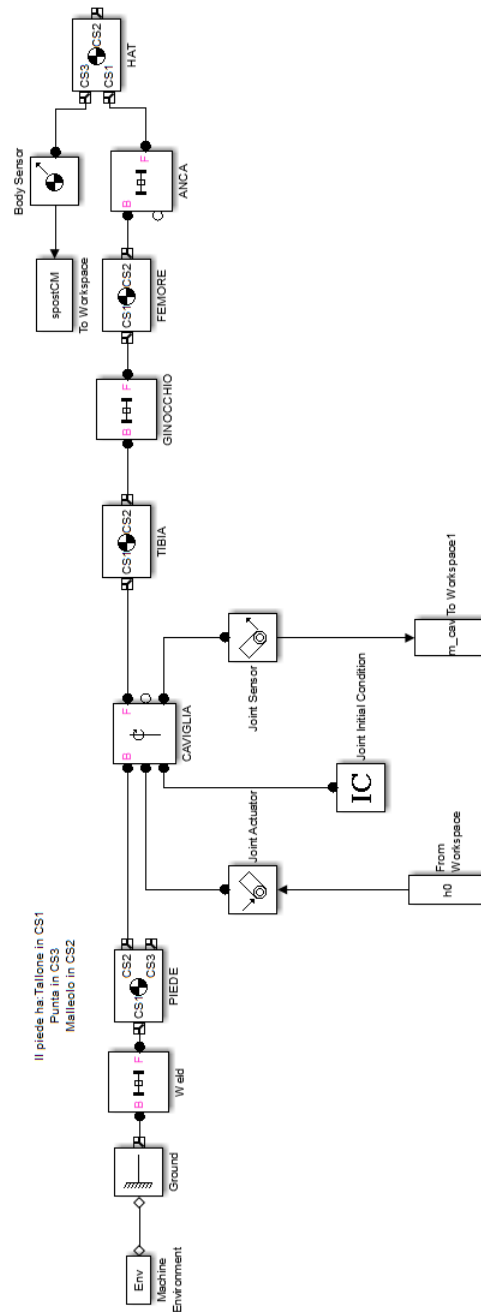


Figure A.2: Simulink Block Diagram

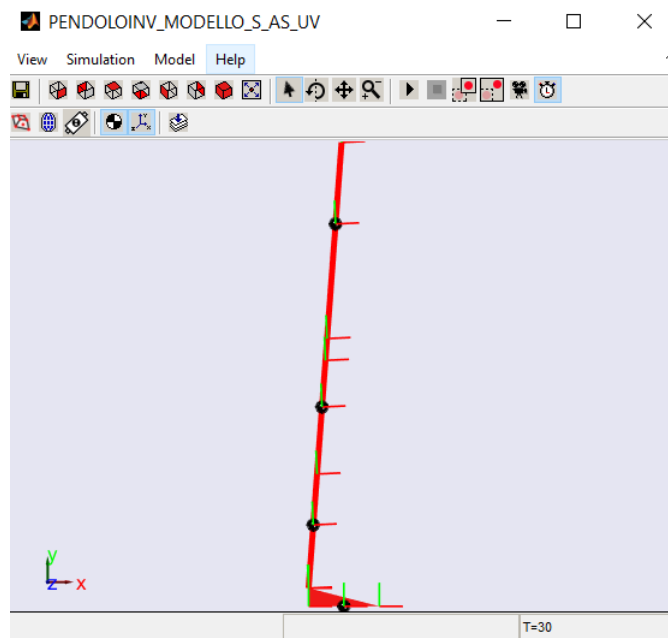


Figure A.3: Simulink Simulation front panel

Appendix B

Software

B.1 Smart Capture

Smart Capture is an acquisition software that manages the optoelectronic system, force plates and electromyographes of BTS S.p.A.([BTS](#)). The systems can be acquired stand alone or synchronously. In our application is possible to set a trigger signal in output to synchronize it, trough a trigger box, with other external instrumentation, in particular with the image acquisition system.

The procedure for each record requires to reset the force plate with no force applied on (data acquisition function 'Monitor') and then start the recording session (function 'Acquisizione'), then after finishing the session, it is necessary to save the data in a proprietary format, exportable in text files. In figure [B.1](#) a general image of the user interface is presented

B.2 Sopera CamExpert

The CamExpert Sopera software is a software that manages the grabber board, the Xcelera-CL_PX4.1, and the camera, it supports many camera models and producers, we used the Dalsa Falcon.

There are many tabs in the Front panel to input the parameters of acquisition. In figure [B.3](#) are shown the basic timing parameters, the advanced controls, the

B.2 Sapera CamExpert

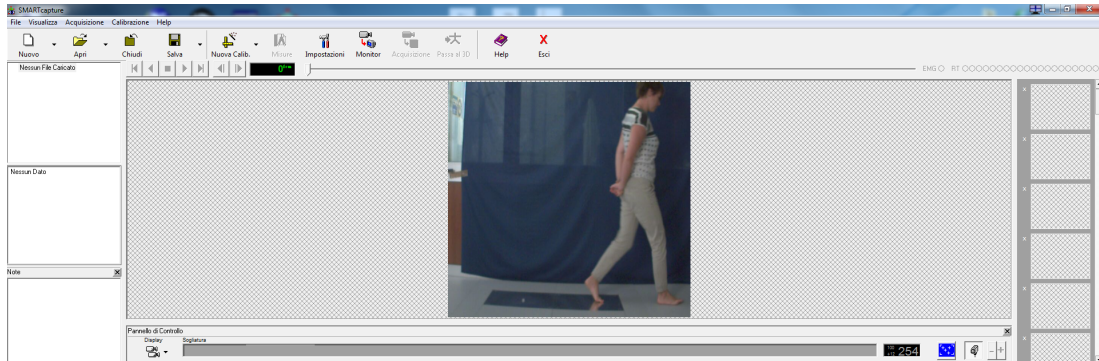


Figure B.1: Smart Capture - Reference camera recording

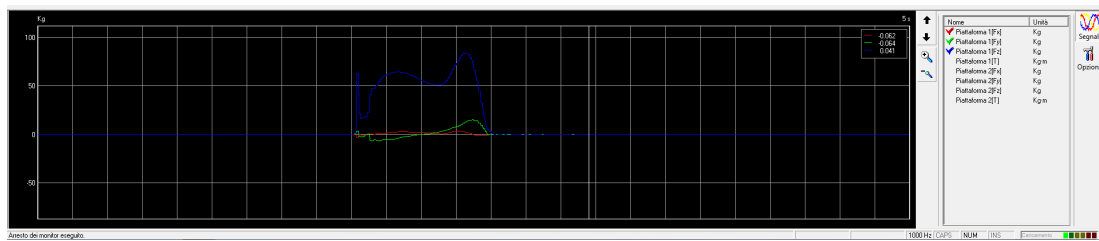


Figure B.2: Smart Capture - Force Platform

external trigger parameters and the image buffer.

When the parameters are set it is possible to create a configuration file (File-Save as), to save and make the configuration settings available for others application.

B.2 Spera CamExpert

Camera Information Parameters	
Parameter	Value
Camera Model	FA-20-01M1H-00-R
Firmware Version	24274
Active Load Version	1.0.1.134
Camera Serial	18000010
Baud Rate	115200
Power-Up Configur...	Setting...
Error Report	Wizard...
PoCL	Disabled
PoCL Status	Not Active

Camera Control Parameters	
Parameter	Value
Sensor Width (in Pix...	1400
Sensor Height (in Li...	1024
Sensor Left Offset (i...	0
Sensor Top Offset (i...	0
Frame Rate (Hz)	100.0
Camera Link Mode	3 (10 bits)
System Gain	1024
Digital Offset (DN)	0
Subtract Backgroun...	0
Exposure Control	Setting...
Enable Flat Field Cor...	Enable FPN and PRNU
Flat Field Correction	Setting...
Binning Horizontal	Disabled
Binning Vertical	Disabled
Mirroring Mode	Disabled
Output Throughput...	160
Test Image Selector	Video

(a) Basic camera communication parameter.

(b) Advanced camera image parameters.

External Trigger Parameters	
Parameter	Value
External Trigger	Enable
External Trigger Det...	Falling Edge
External Trigger Level	RS-422
External Trigger Sou...	Automatic
External Trigger Min...	0
Frame Count per Ext...	1

Image Buffer and ROI Parameters	
Parameter	Value
Image Width (in Pix...	1392
Image Height (in Li...	1024
Image Left Offset (i...	0
Image Top Offset (i...	0
Image Buffer Format	Monochrome 16-bits

(c) Camera synchronization.

(d) Camera image format.

Figure B.3: Spera Cam expert software.

B.3 Acquisition software

Image acquisition software has been developed in Matlab.([Matlab](#)) Our software has to be used both in synchrony with the force plates and stand alone, as shown in 4.2, for video acquisition. The graphic user interface is shown in figure B.4.

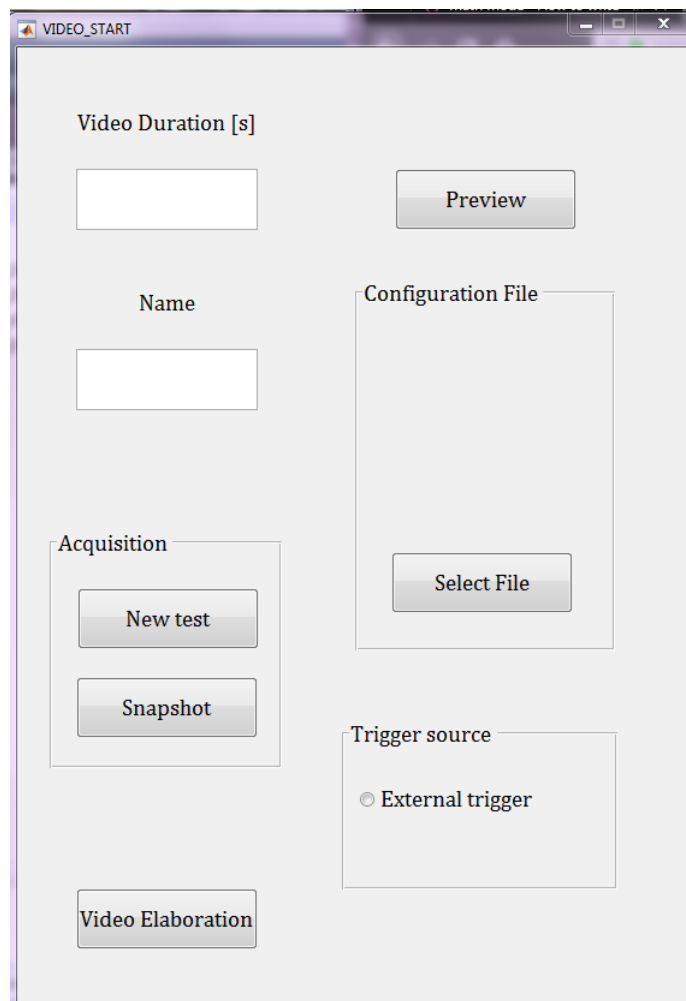


Figure B.4: Front panel of the acquisition software

The user has to compile the empty field with the duration and the record name of the video. If the user doesn't change the name field, the software automatically increase the number of the name each time the button 'New test' is pressed.

Example:

Name: Walking

VideoName : Walking_0 \Rightarrow *button 'New test' pressed* \Rightarrow *VideoName : Walking_1*

Depending on the specification of the test that is being filmed, in peculiar velocity and light conditions, it is necessary to set some parameters of the Dalsa camera we are using.

As described in section [B.2](#), according to camera settings Sopera software produce a configuration file that has to be loaded by the software to set camera options. Through the button 'Configuration File' it is possible to select the required configuration file, if none is chosen, a default one is loaded and its name displayed in the box.

As said before, the trigger source has to be set, it can either be 'Automatic' or 'External': in the first case the acquisition starts as the button 'New test' is pressed; in the second case when the button is pressed a message pops up on the screen saying 'Camera Ready' and the program waits the trigger signal from the external circuit.

Settings have been set according to the output of the force plates software, specifically it is a 'Falling edge' trigger signal. As mentioned in chapter [4 4.3](#)

As the acquisition finishes the software asks the user whether to save the video or not. This functionality has been added not to waste time and memory space in saving videos of big dimensions, if errors or criticalities are already known by the user.

'Preview' button let the user to have a preview of the video output of the camera, without saving any file.

'Snapshot' button takes an image from the camera and saves it with the name inserted in the 'Name' field.

B.4 Elaboration software

The elaboration algorithm takes as a inputs:

- . The video recorded in lossless 'avi' format;
- . The number of markers applied, depending on the protocol used;
- . The treshold for the conversion from grayscale to black and white;
- . The sensitivity value in pixel/mm obtained from calibration procedure;

and provides as output the markers' trajectory in time. [B.5](#)



Figure B.5: Flow diagram of elaboration software

The elaboration is a loop in which each frame of the 'avi' file is elaborated. The first frame is converted in black and white, then there is a research of white regions and its weighted centroid. That is a good approximation of the effective position of the marker, considering the light diffusion from the led and the gray levels on the image.

At this point it is requested the input of the user, to select the identity of each marker, assigning to it a number.

If in the first frame there are not enough markers, due to an error or occlusion, it is possible to select a subsequent frame.

For the next frames the elaboration develops in a nested loop. For each frame and each marker the position is searched in a specific region of interest, ROI.

The region of interest where the next marker position is searched is calculated making some assumptions: we start from the previous position, we assume a new position based on velocity calculated from the two previous position, and then we create an area with a certain number of pixels.

Now we have three possible situations:

1. There is a marker in the ROI;
2. There is not only a marker in the ROI;

3. There is no marker in the ROI;

In the first case the position is assumed and the loop ends, the elaboration goes to another marker.

In the second case the user is asked to choose, with a graphic input the right marker position, if there are any reflexions or markers very near to each other. Even manual selection can be difficult and eventually erroneous.

In the third case the ROI automatically enlarge its bounds twice, tries to find the marker and repeat the operation for four times, if this procedure doesn't find the marker, the user is asked to examine the image and to select if the marker is completely lost or still out of the inspected region. If the answer is the loss of a marker, previous value is assigned and the loop ends, if the markers is 'Out of region' the user has to select the center of the new region manually, then the software finds the marker in the new ROI by itself.

Knowing the position of the marker we can then calculate velocity, used in the loop to find the region of interest in the next frame.

When the inner loop for the first marker, is finished the software checks the distance from a marker to another, to find if there is a superposition, if that is the case it asks the user to select manually the identity of the marker.

When a marker is lost, there can be mainly two approaches. It is possible to interpolate the value of the position or to leave the previous value as an indication of error, it depends on user intention, to correct or underline the presence of an error and the consequential unreliability of that measurement.

The algorithm then takes the positions in pixels and converts them in millimeters, it smooths the positions, calculates the velocities and accelerations with a Savitzky-Golay filtering procedure, respectively of zero, first and second order. Finally it names the markers as selected by the user and then saves the results in a '.mat' file.

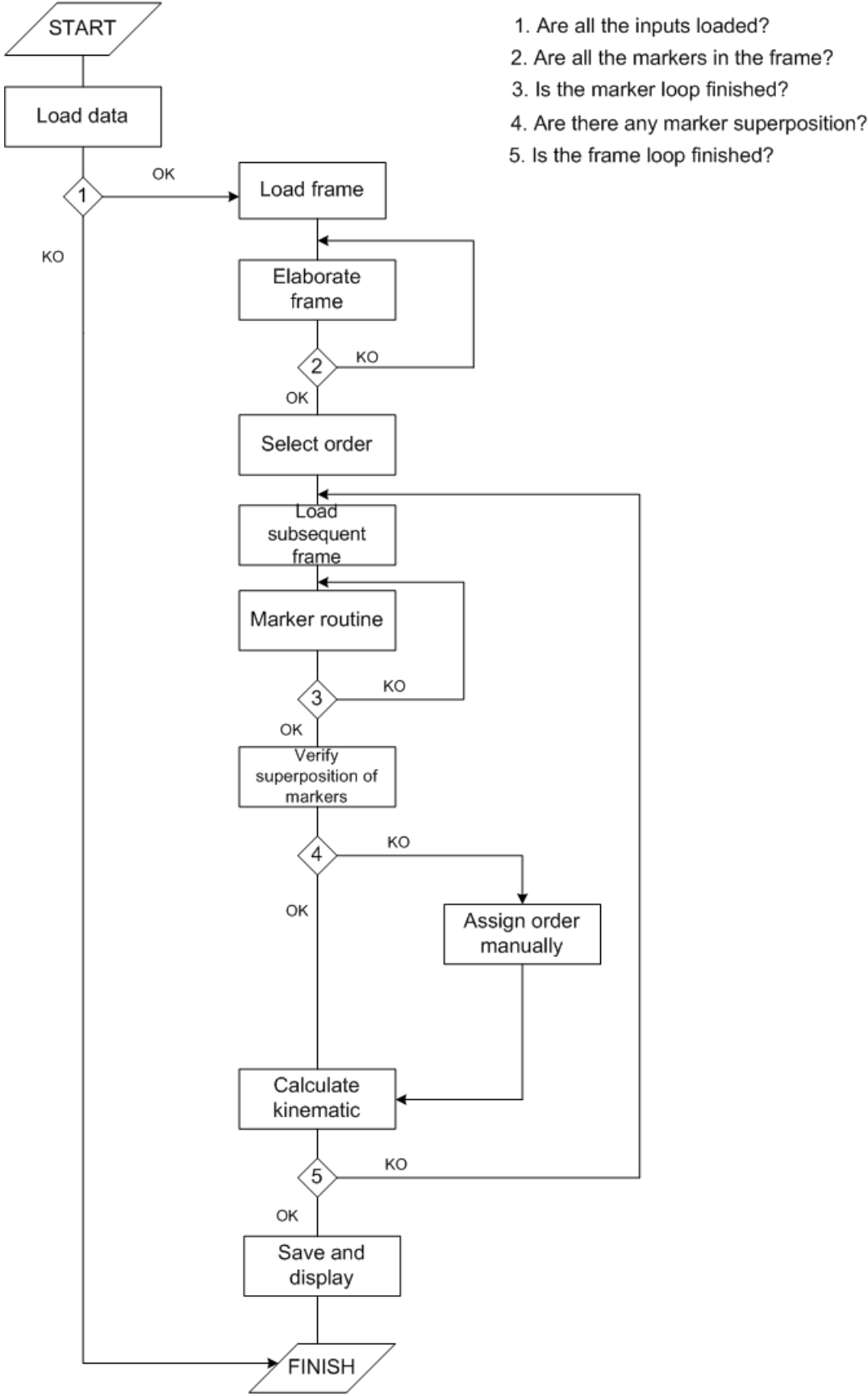


Figure B.6: Marker tracking flow diagram

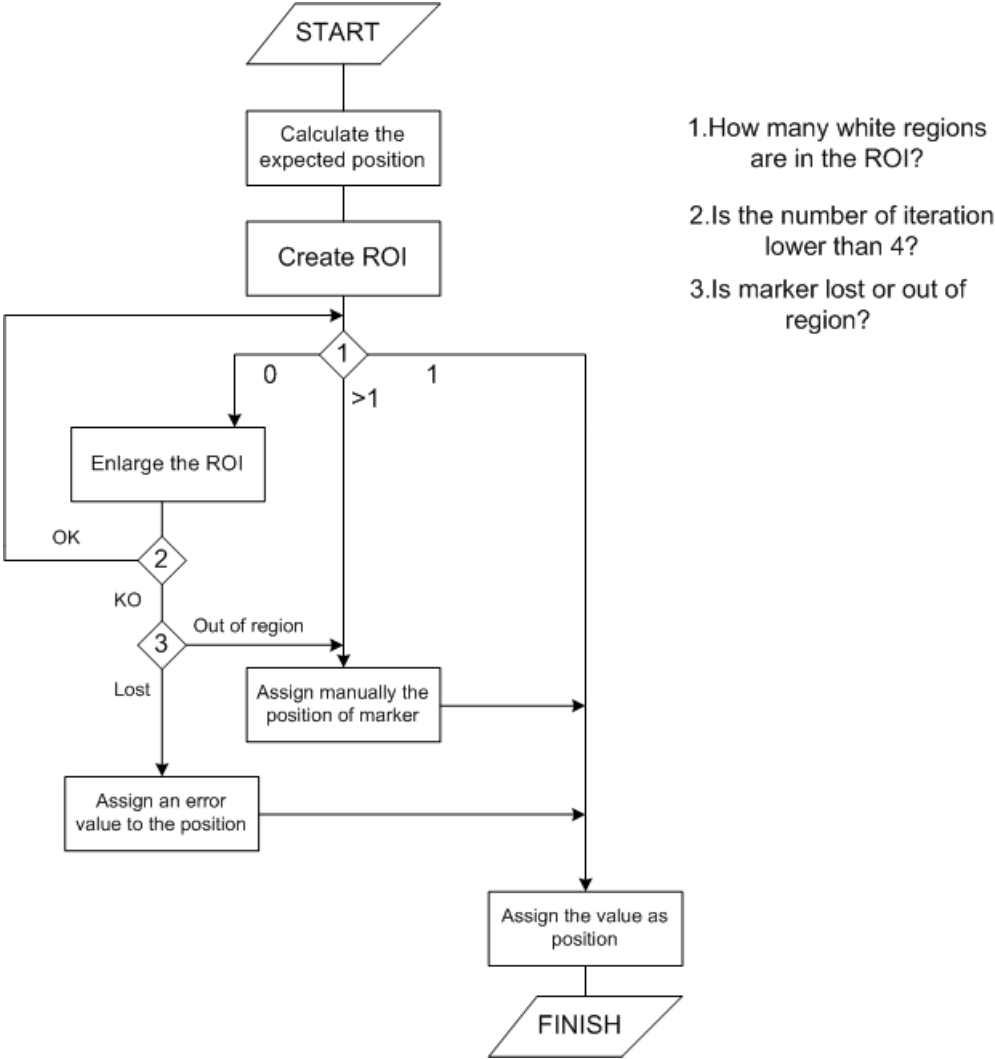


Figure B.7: Marker routine flow diagram

References

- [1] BOONSTRA, T.A., SCHOUTEN, A.C. & VAN DER KOOIJ, H. (2013). Identification of the contribution of the ankle and hip joints to multi-segmental balance control. *Journal of NeuroEngineering and Rehabilitation*, **10**.
- [BTS] BTS (2018). Bts s.p.a., milano, italy. <https://www.btsbioengineering.com/it/>, accessed: 13-10-2018.
- [2] CARLOCK, J. (2004). The relationship between vertical jump power estimates and weightlifting ability: a field-test approach. *Strength and conditioning J*, **18**.
- [3] CHANDLER T.J., S. (1991). The squat exercise in athletic conditioning. *Strength and conditioning J*, **1**.
- [4] CHIMERA, N.J., SWANIK, K.A., SWANIK, C.B. & STRAUB, S.J. (2004). Effects of plyometric training on performance in female athletes. *Journal of Athletic Training*, **39**, 24–31.
- [5] CRENNNA, F., ROSSI, G. & PALAZZO, A. (2015). Measurement of human movement under metrological controlled conditions. *Acta IMEKO*, **4**, 48–56.
- [6] CRENNNA, F., ROSSI, G.B. & PALAZZO, A. (2016). Instantaneous centre of rotation in human motion: measurement and computational issues. *Journal of Physics: Conference Series*, **772**.
- [7] CRENNNA F., B.V.P.A., ROSSI G.B. (2015). Filtering signals for movement analysis in biomechanics. *Proc XXI IMEKO World Congress*, **5**.
- [8] CRENNNA F., R.G., PALAZZO A. (2018). Ankle moment measurement in biomechanics. In *Imeko XXII World congress*, Belfast, Ireland.
- [9] CRENNNA F., R.G., PALAZZO A. (2018). Power measurement in maximum height jump. In *Imeko XXII World congress*, Belfast, Ireland.

REFERENCES

- [10] CRÉTUAL, A. (2015). Which biomechanical models are currently used in standing posture analysis? *Neurophysiologie Clinique*, **45**, 285–295.
- [11] CROCE, U.D., LEARDINI, A., CHIARI, L. & CAPPOZZO, A. (2005). Human movement analysis using stereophotogrammetry: Part 4: assessment of anatomical landmark misplacement and its effects on joint kinematics. *Gait and Posture*, **21**, 226 – 237.
- [12] D, E. (2011). Power mechanics for power lifters. *Sandro Ciccarelli*, 171.
- [13] D.A., W. (2015). *Biomechanics and motor control of human movement*. Wiley.
- [14] DUGAN E.L, D.T.E.A. (2004). Determining the optimal load for jump squats: a review of methods and calculations. *Strength and conditioning J*, **18**.
- [ETH] ETH (2018). Eth website. <https://www.ethz.ch/content/specialinterest/baug/institute-ibk/structural-mechanics/en/education/identification-methods-for-structural-systems.html>, accessed: 13-10-2018.
- [15] FORTENBAUGH, D., SATO, K. & HITT, J. (2010). The effects of weight lifting shoes on squat kinematics. *SOURCE International Symposium on Biomechanics in Sports: Conference Proceeding*, **28**, 1.
- [16] FUJISAWA, N., MASUDA, T., INAOKA, H., FUKUOKA, Y., ISHIDA, A. & MINAMITANI, H. (2005). Human standing posture control system depending on adopted strategies. *Medical and Biological Engineering and Computing*, **43**, 107–114.
- [17] GAWTHROP, P., LORAM, I., LAKIE, M. & GOLLEE, H. (2011). Intermittent control: A computational theory of human control. *Biological Cybernetics*, **104**, 31–51.
- [18] HERMENS H.J., M.R.E.A. (1999). *European Recommendations for surface electromyography*. Roessingh Research and Development.
- [19] HERMENS H.J., M.R.E.A. (1999). *The state of the art on signal processing methods for surface electromyography*. Roessingh Research and Development.
- [20] KADABA, M.P., RAMAKRISHNAN, H.K. & WOOTTEN, M.E. (1990). Measurement of lower extremity kinematics during level walking. *Journal of Orthopaedic Research*, **8**, 383–392.

REFERENCES

- [21] KARLSSON, A. & PERSSON, T. (1997). The ankle strategy for postural control - A comparison between a model-based and a marker-based method. *Computer Methods and Programs in Biomedicine*, **52**, 165–173.
- [22] KIM, K.J., AGRAWAL, V., BENNETT, C., GAUNAURD, I., FEIGENBAUM, L. & GAILEY, R. (2018). Measurement of lower limb segmental excursion using inertial sensors during single limb stance. *Journal of Biomechanics*, **71**, 151–158.
- [23] KLAVORA, P. (2000). Vertical-jump Tests : A Critical Review. *Strength and conditioning J*, **22**.
- [24] L., L. (1987). *System identification theory for the user*. Prentice-Hall.
- [25] LEARD J.S., K.E.A., CIRILLO M.A (2007). Validity of two alternative systems for measuring vertical jump height. *Strength and conditioning J*, **21**.
- [26] LEARDINI, A., CHIARI, L., CROCE, U.D. & CAPPOZZO, A. (2005). Human movement analysis using stereophotogrammetry: Part 3. soft tissue artifact assessment and compensation. *Gait and Posture*, **21**, 212 – 225.
- [27] LEGNANI G., F.I., PALMIERI G. (2018). *Introduzione alla biomeccanica dello sport*. Città Studi.
- [28] LENZI, D., CAPPELLO, A. & CHIARI, L. (2003). Influence of body segment parameters and modeling assumptions on the estimate of center of mass trajectory. *Journal of Biomechanics*, **36**, 1335–1341.
- [29] LINTHORNE, N.P. (2001). Analysis of standing vertical jumps using a force platform. *American Journal of Physics*, **69**, 1198–1204.
- [30] LORAM, I.D. & LAKIE, M. (2001). Balancing of an inverted pendulum: subject sway size is not correlated with ankle impedance. *Ispg*, 298.
- [31] LORAM, I.D. & LAKIE, M. (2002). Direct measurement of human ankle stiffness during quiet standing: The intrinsic mechanical stiffness is insufficient for stability. *Journal of Physiology*, **545**, 1041–1053.
- [32] LUTZ G., E.A., PALMITER R (2003). Comparison of tibiofemoral joint forces during open-kinetic-chain and closed-kinetic-chain exercises. *Strength and conditioning J*, **26**.
- [33] MADDIGAN M.E., B.D. & D.G., B. (2014). Lower-limb and trunk muscle activation with back squats and weighted sled apparatus. *Strength and conditioning J*, **28**.

REFERENCES

- [Matlab] Matlab (2018). Matlab website. <https://it.mathworks.com/products/matlab.html>, accessed: 13-10-2018.
- [34] MAURER & PETERKA (2005). A new interpretation of spontaneous sway measures based on a simple model of human postural control. *Journal of Neurophysiology*, **93**, 189–200.
- [35] MEULEMAN, J.H., VAN ASSELDONK, E.H. & VAN DER KOOIJ, H. (2013). The effect of directional inertias added to pelvis and ankle on gait. *Journal of NeuroEngineering and Rehabilitation*, **10**, 1–12.
- [36] M.F.BOBBERT, K. (1996). Why is countermovement jump height greater than squat jump height? *Medicine and Science in Sports Exercise*, **1**.
- [37] MORASSO, P.G. & SANGUINETI, V. (2002). Ankle muscle stiffness alone cannot stabilize balance during quiet standing. *Journal of Neurophysiology*, **88**, 2157–2162.
- [38] NEMA, S., KOWALCZYK, P. & LORAM, I. (2015). Complexity and dynamics of switched human balance control during quiet standing. *Biological Cybernetics*, **109**, 469–478.
- [39] NIGG B.M., H.W. (1999). *Biomechanics of the musculo-skeletal System*. Wiley.
- [40] NISTI, A. (2015). Algorithms for controlling and tracking uavs in indoor scenarios. <https://github.com/andrea-nisti/algorithms-controlling-tracking>, accessed: 13-10-2018.
- [41] OHIRA, T. & UZAWA, T. (2015). *Mathematical Approaches to Biological Systems*. Springer.
- [OpenSim] OpenSim (2018). Opensim website. <http://opensim.stanford.edu/>, accessed: 13-10-2018.
- [OpeSimDocumentation] OpeSimDocumentation (2018). Opensim documentation. <https://simtk-confluence.stanford.edu/display/OpenSim/Getting+Started>, accessed: 13-10-2018.
- [Optitrack] Optitrack (2018). Optitrack website. <http://www.optitrack.com/>, accessed: 13-10-2018.
- [42] PALAZZO A., R.G., CRENNNA F. (2018). Dynamic simulation of auto-oscillating sway posture. In *8th World Congress of Biomechanics*, Dublin, Ireland.

REFERENCES

- [43] POWERS (1996). Vertical jump training for volleyball. *Strength and conditioning J*, **18**.
- [44] RILEY, H., MANN (1990). Modelling of the biomechanics of posture and balance. *Journal of Biomechanics*, **23**.
- [45] SARGENT, D. (1921). The physical test of man. *Ann Physical Education Review*, **26**.
- [46] SCHOENFELD, B. (2010). Squatting kinematics and kinetics and their application to exercise performance. *Strength and conditioning J*, **24**.
- [47] SEIREG, A. & ARVIKAR, R. (1975). The prediction of muscular load sharing and joint forces in the lower extremities during walking. *Journal of Biomechanics*, **8**, 89 – 102.
- [Simulink] Simulink (2018). Simulink website. <https://it.mathworks.com/products/simulink.html>, accessed: 13-10-2018.
- [48] SMITH, A.W. & WONG, D.P. (2012). Effects of window size on ankle joint stiffness calculation during quiet standing: How the rule changes the result. *Journal of Biomechanics*, **45**, 2301–2305.
- [49] SUZUKI, Y., NOMURA, T., CASADIO, M. & MORASSO, P. (2012). Intermittent control with ankle, hip, and mixed strategies during quiet standing: A theoretical proposal based on a double inverted pendulum model. *Journal of Theoretical Biology*, **310**, 55–79.
- [SYS] SYS (2018). System identification toolbox. <https://it.mathworks.com/products/sysid.html>, accessed: 13-10-2018.
- [50] TISEO, C., ANG, W.T. & SHEE, C.Y. (2015). Dynamics of the mobile robotic balance trainer: Study of the pentagonal closed chain properties in relation with balance tasks. *IEEE International Conference on Rehabilitation Robotics*, **2015-September**, 753–757.
- [Vicon] Vicon (2018). Vicon website. www.vicon.com, accessed: 13-10-2018.
- [51] WINTER, D.A. (1995). Human balance and posture control during standing and walking. *Gait & posture*, **3**, 193–214.
- [52] WISLØFF, U., CASTAGNA, C., HELGERUD, J., JONES, R. & HOFF, J. (2004). Strong correlation of maximal squat strength with sprint performance and vertical jump height in elite soccer players. *British Journal of Sports Medicine*, **38**, 285–288.

REFERENCES

- [53] WU, G. & CAVANAGH, P.R. (1995). Isb recommendations for standardization in the reporting of kinematic data. *Journal of Biomechanics*, **28**, 1257 – 1261.
- [54] ZIV, G. & LIDOR, R. (2010). Vertical jump in female and male basketball players-a review of observational and experimental studies. *Journal of Science and Medicine in Sport*, **13**, 332–339.